Compressive Strength Prediction of High Early Strength Concrete: An Integrated Framework of Artificial Neural Network and Genetic Algorithm Based Approach

By

Muhammad Imran

MS-2019-00000-320799

Supervisor

Dr. Rao Arsalan Khushnood

NUST INSTITUTE OF CIVIL ENGINEERING

SCHOOL OF CIVIL AND ENVIRONMENTAL ENGINEERING

NATIONAL UNIVERSITY OF SCIENCES AND TECHNOLOGY

H-12, ISLAMBAD

2022

This is to certify that

Postgraduate Thesis titled

Compressive Strength Prediction of High Early Strength Concrete: An Integrated Framework of Artificial Neural Network and Genetic Algorithm Based Approach

Submitted By

Muhammad Imran 00000320799

has been accepted towards the

requirements for a postgraduate degree

in

STRUCTURAL ENGINEERING

_____

Dr. Rao Arsalan Khushnood

Assistant Professor

NUST Institute of Civil Engineering

School of Civil and Environmental Engineering

National University of Sciences and Technology, Islamabad, Pakistan

THESIS ACCEPTANCE CERTIFICATE

Certified that the final copy of MS/MPhil thesis written by Muhammad Imran, Registration No. 00000320799, of MS Structural Engineering 2019 Batch (NICE) has been vetted by the undersigned, found completed in all respects as per NUST Statutes/Regulations, is free of plagiarism, errors, and mistakes and is accepted as partial fulfillment for the award of MS/MPhil degree. It is further certified that necessary amendments as pointed out by GEC members of the scholar have been incorporated in the said thesis.

Name of Supervisor: _____

Signature: _____

Date: _____

Signature (HoD): _____

Date: _____

Signature (Dean/Principle): _____

Date: _____

Dedication

“This work is dedicated to my caring and loving parents and teachers who have been supportive throughout the degree”

Acknowledgment

All praises are to Allah, the Most Merciful, and blessing to Muhammad (S.A.W). It is due to Almighty Allah's infinite bounties which I was able to complete my thesis.

Several people helped throughout the completion of this thesis. First and foremost, I want to express my gratitude to our beloved parents and instructors for their unwavering love and support throughout our lives, as well as for inspiring us to pursue our aspirations.

I'd like to thank Assistant Professor Dr. Rao Arsalan (NICE), for his direction and support during the research. I owe him thanks for keeping me going on this difficult path. Throughout the endeavor, he spent many hours reflecting, reading, encouraging, and most importantly, keeping me on the right path of research with patience. I am extremely grateful to PG students Engr. Zahid Ullah (SCME, NUST) and Engr. Muzammil Khan (SCME, NUST) for their great help to me in understanding the machine learning concepts, writing MATLAB codes, and extracting results.

In addition, I am grateful to Dr. Hammad Anis, Dr. Muhammad Azam Khan, and Lecturer Arsalan Mushtaq of my Guidance and Examination Committee (GEC) for their invaluable advice. Furthermore, contributions from other students are also recognized.

TABLE OF CONTENTS

Figures List

Tables List

List of Abbreviations

ANN	Artificial Neural Network
BEP	Burned Eggshell Powder
C_Type	Cement Type
CEM I 42,5N*	Normal Strength 42,5 Class
CEM I 52,5N*	Normal Strength 52,5 Class
CEM I 42,5R*	High Early Strength 42,5 Class
CEM I 52,5R*	High Early Strength 52,5 Class
CSA	Calcium Sulphoaluminate
EP	Eggshell Powder
ET	Ensemble Tree
FAF	Fly Ash Class-F
GA	Genetic Algorithm
GBA	Ground Bagasse Ash
GEP	Gene Expression Programming
GGBFS	Ground Granulated Blast Furnace Slag
GPR	Gaussian Process Regression
HESC	High Early Strength Concrete
LASA	Low Alkali Sulpho Aluminate
LF	Limestone Filler
MA1	Mineral Admixture-1
MA2	Mineral Admixture-2
MAE	Mean Absolute Error
MK	Metakaolin
ML	Machine Learning
MLR	Multi Linear Regression
MSE	Mean Square Error
NCSHC	Nano CSH Crystals
NCuO	Nano CuO
NCuZnF	Nano CuZn Ferrite
NFe2O3	Nano Fe2O3
NMC	Nano Metaclay
NNiF	Nano Ni Ferrite
NS	Nano Silica
PIA	Processed Incineration Ashes
RMSE	Root Mean Square Error
R	Coefficient of Relation
R^2	Coefficient of Determination
SAP	Superabsorbent Polymer
SF	Silica Fume
SVM	Support Vector Machine

ABSTRACT

Compressive strength of high early strength is related non-linear with its components. In order to effectively utilize the high early strength concrete, compressive strength estimation is necessary. Nowadays, compressive strength prediction is done by a lot of researchers using machine learning tools with acceptable accuracy and performance. Therefore, in this research, an integrated framework of genetic algorithms and artificial neural networks was proposed. The compiled data consisting of eleven input and one output variable was used to train the model. The developed model has shown a high accuracy with a correlation coefficient of around 0.98 and a mean absolute error close to 3. Feature importance demonstrated that cement and water-binder ratio are the top two candidates contributing to the model whereas partial dependence plot analysis showed output variation with inputs. The comparison with other in-practiced machine learning techniques showed that the developed model has the highest performance. In addition, the lab-scale experiments further provided an evaluation of the model and displayed those results from the model and actual are close to the 5 percent error.

Key Words:

Compressive Strength, Machine Learning, Optimization, High Early Strength Concrete

Chapter 1

INTRODUCTION

1.1 General

The most widely applied construction material is concrete in buildings, bridges, and structures. The main ingredient of concrete consists of aggregate, water, and cement. Research has been focused on alternative cementitious materials due to a huge portion of the carbon dioxide released in the production of cement. Around 5-8 percent of global CO_2 emitted come from the cement industry [1]. In addition, normal concrete is not considered good for special properties like higher abrasion resistance, higher initial strength, higher flowability, greater ultimate strength, and higher durability [2]. In this regard, high-performance concrete (HPC) is playing a key role to decrease the environmental impact of cement which also have better properties as well which are prepared using additional cementitious materials. According to their properties, these concretes are divided into many categories. Furthermore, normally, superplasticizers are utilized to diminish the effect of the low water to cement ratio [3].

1.2 High Early Strength Concrete

High early strength concrete is a type of high-performance concrete that achieves its designated compressive strength before time. It is also famous for fast-track construction and a minimum one-day specified strength is usually 17 MPa. High early strength is attributed to both high early and high strength concrete. [3-5]. High initial strength is utilized by designers to design efficient structures. Both normal and special concrete components are utilized to prepare HESC. There are several advantages of HESC, but most notable are higher early compressive strength, fast cast-in-place construction, speedy paving, enhanced precast elements production, fast-track repairing of pavements, accelerated usage of formwork and concreting in cold weather areas [3].

Furthermore, the COVID-19 calamity has affected all of the important sectors like agriculture, education, transportation, health, construction, etc. In order to minimize the effects of COVID-19, infrastructure development became a prime concern at every level, particularly those infrastructures which deal with the medication and health like hospitals, quarantine centers, medical facilities, etc. In this regard, there are many techniques applied for this purpose but in

concrete construction, HESC has a high perspective to fulfill these mentioned challenges, especially in those projects which demand immediate requirements of buildings, transportation, and medical infrastructure. Because of the application of sustainable supplementary cementitious materials, will not only satisfy the need for early infrastructure operations but also reduce the determinantal effects of cement production [6].

a) Prestressed Concrete *b) Fast Track Construction of a Bridge*

Figure 1 Applications of HESC

High early strength concrete can be prepared using various techniques, methods, and materials. Regarding materials variation, mostly high early strength cement, decreased water-binder ratio, increased cement quantity, and special types of cement are used. Additionally, mineral admixtures are also used either in combination with others or alone [3].

Many different types of cement are used to get high early strength, nevertheless, the usage of high early strength and calcium Sulpho aluminate cement are high due to their availability and good performance [7]. High early strength cement is designed to achieve early strength in comparison to normal Portland cement, but it has some drawbacks which include high shrinkage and increased generation of cement heat [8-10]. In addition, normally, normal strength cement 42.5 and normal strength cement 52.5 is used along with mineral admixtures to enhance the early strength because these are easily available and environmental friendly [11, 12].

In the same way, there is another key property of mixtures that plays an important role in the high early strength which is known as the water to binder ratio. In order to achieve high early strength, normally its value is set low which is why in most cases superplasticizers become a key part of the HESC mixtures in order to control heat production and slump reduction [13-

15]. Moreover, high early strength is also affected by changes in both the type and quantity of mineral admixtures. Fly ash and silica fume are the two most widely used mineral admixtures due to their ease of availability and less cost. Many advantages are associated with the use of fly ash which include low permeability, high workability, and reduced heat generation which is effective in controlling decreased slump values because of reduced water binder ratio [16, 17]. Silica fume usage is also wide due to its contribution in both the early and final strength. Silica fume causes pore refinement due to its micro size which enhances the strength of concrete [18]. Likewise, many other mineral admixtures have also been employed to increase the early strength while keeping the environmental challenges low [4, 5, 19].

Different mineral admixtures have also been utilized while combining with others recently in order to increase the early strength. For instance, improved mechanical properties specifically compressive strength have been observed when slag is used in combination with the silica fume. This is due to the reason that slag caters to the low slump issue while silica fume compensated for the reduced early strength [18, 20]. Furthermore, nowadays, nano materials have also been extensively applied to enhance the early compressive strength of concrete either separately or while combining with other mineral admixtures. These increase compressive strength and durability because of pore refinement of concrete skeleton due to their nano size [13, 21]. This is shown in various experiments that improved early compressive strength along with the enhanced durability and mechanical properties obtained when different nano materials are used in concrete [22, 23]. The most widely employed nano material for enhanced properties of concrete is nano-silica and several researchers have applied it to improve the early compressive strength [15, 24].

Chapter 2

REVIEW OF LITERATURE

2.1 Applications of Machine Learning in Civil Engineering

Even though high early strength concrete has been prepared with a variety of materials and a lot of experimental research has been done on it, the experimental procedure adopted for this is highly resource and time-consuming. The experimentation also takes a lot of iteration which generates a lot of waste materials and makes this process costly. Due to these limitations, the use of HESC has been limited. Consequently, there is a great need for a soft tool that can give an accurate estimate of the HESC compressive strength without going through this labor-intensive and costly experimentation.

Machine learning which is a subgroup of artificial intelligence (AI) has emerged as a breakthrough for the prediction of properties for various engineering materials based on past data. These data-driven ML models are also playing a key role in the concrete industry for estimating a variety of concrete properties like flexural strength [25], tensile strength [26], modulus of elasticity [26, 27], slump [28], and split tensile strength [29]. Similarly, compressive strength of different kinds of concrete has also been modeled using a variety of ML tools techniques which include but are not limited to support vector machine, decision tree, multilinear regression, artificial fuzzy neural network, random forest, gaussian process regression, artificial neural network, genetic programming [30-34].

2.2 Modelling Methods

A lot of research has been carried out to find the most important parameter of High-Performance Concrete which is compressive strength. Yeh et al. (1998) [35] were the first to use artificial neural networks to build models for the compressive strength prediction of concretes containing fly ash and blast furnace slag. The correlation values obtained between predicted and actual values were strong with the best R = 0.96. Following that, a slew of subsequent studies used Yeh's data to build compressive strength models using various methodologies. In this regard several researchers for example Han et al., Kaloop et al., Anyaoha et al., Chakraborty et al., and Hameed et al. all used the same data to construct unique modeling

methods in this area. Han et al. (2019) [36] utilized 5 input variables built as a result of a difficult variable combination, to develop the random forest algorithm for strength prediction. The high correlation coefficient (R = 0.97) indicates that the developed method was robust and error-free.

Anyaoha et al. (2020) [37] introduced a novel boosting smooth transition regression tree (BooST) model and a comparison with other existing models has also been performed. With a regression coefficient of 0.95, the model's results demonstrated that the proposed model outperformed all others in terms of regression coefficients and error indices. Furthermore, Kaloop et al. (2020) [38] investigated the gradient tree boosting machine (GBM) model for improved predictability of HPC compressive strength by employing 8 distinctive variables. Figure 2 depicts the overall's technique, in which data is first standardized and then trained using several models. With a high coefficient of correlation and small error, the results showed that prediction accuracy was good.

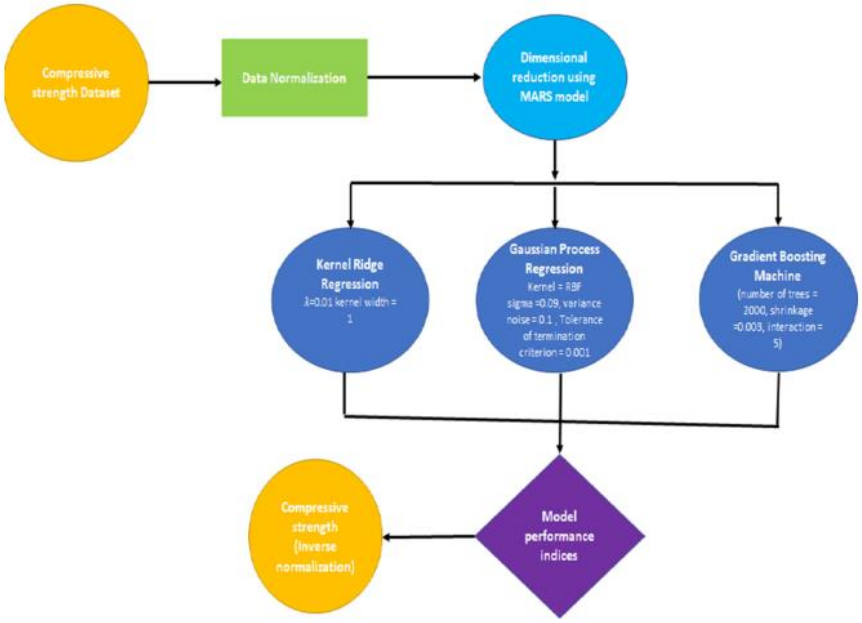

Figure 2 Kaloop et al. [38] overall methodology followed

Chakraborty et al. in 2021 [39] used an extreme gradient boosting strategy to estimate compressive strength using six input variables. Figure 3 depicts the innovative approach used by Chakraborty et al., which shows that feature selection, as well as hyperparameter optimization, were undertaken for improved model performance. With a model correlation

coefficient of 0.97, the model offers the most accurate predictions when compared to previously published models.

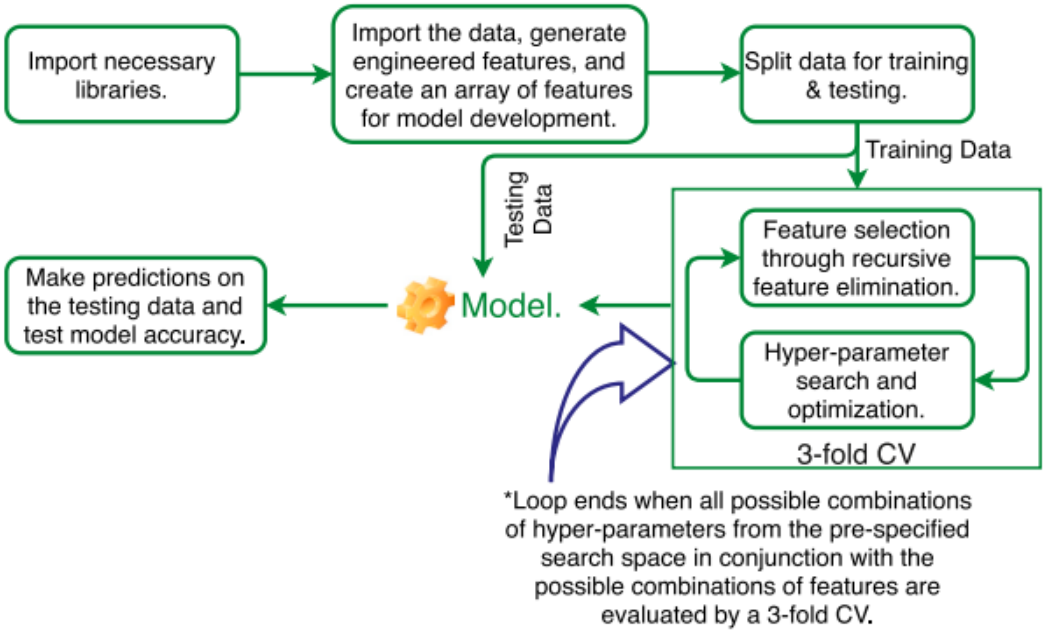

Figure 3 Process of feature selection and optimization by Chakraborty et al. [39]

Similarly, in 2021, Hameed et al. [40] developed the ANN model, which uses 8 input variables and integrates principal component analysis (PCA). The variables are recreated before model training using the PCA, as illustrated in Figure 4, to increase the model's efficiency. The output of the model showed a high level of agreement between expected and actual values (R = 0.96).

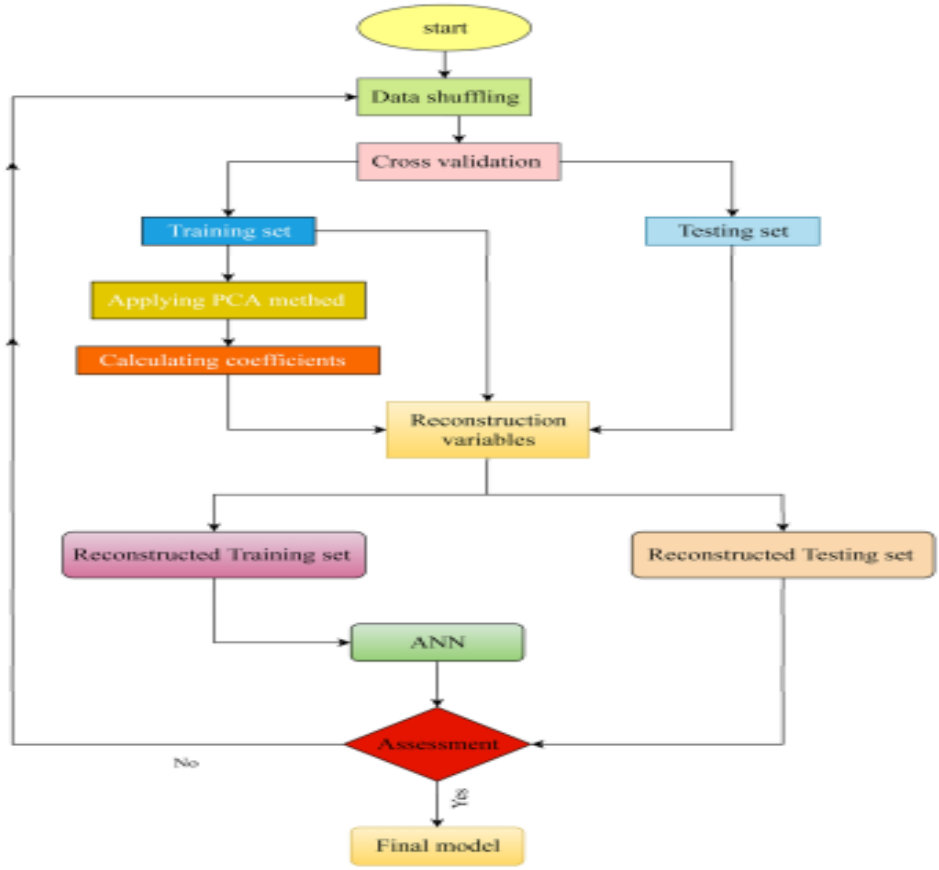

Figure 4 Framework adopted by Hameed et al. [40]

Only a few studies have created datasets that can be used for predictive modeling. Hoang et al. [41], for example, used the gaussian process regression to simulate the compressive strength of high-performance concrete (GPR). The study employed 239 data points from the experimental testing of HPC samples with 7 important influencing parameters. In terms of prediction, the proposed model had superior performance (R = 0.94) when compared with support vector machine and neural network models.

Moreover, just a few academics have used optimization methods to improve machine learning systems' prediction abilities. Yu et al. [42], for example, created an expert approach for improving model performance by combining a support vector machine with enhanced cat swarm optimization (ECSO). The proposed optimized support vector machine model outperformed other conventional models in terms of predictive ability and accuracy.

Furthermore, Bui et al. [43] produced an artificial neural network model that was improved using a novel and adaptive firefly algorithm, and the model's performance was excellent (R = 0.95). Between 2020 and 2022, Golfashani et al. [2, 44] presented two new techniques. The

grey wolf optimizer (GWO) was combined with an efficient neural network type i.e., ANFIS and ANN, in the first approach to improve the models' prediction capacity. While Harris hawk's optimization was hybridized with radial basis and multi-layer networks, in the second approach. Both methodologies were capable to establish significant predictability based on statistical metrics and can be used to accurately estimate the compressive strength of high-performance concrete.

To the author’s knowledge, no study has focused to anticipate High Early Strength Concrete’s compressive strength. Furthermore, the majority of investigations have not given consideration to many categories that may influence compressive strength. Furthermore, no Genetic Algorithm has been combined with an Artificial Neural Network to improve the prediction efficiency of ANN. Finally, in the previous papers, experimental verification of presented models was mostly overlooked.

An efficient ANN-GA model in this study is created as a result of the aforementioned gaps. GA has been used to pick the best architecture for the ANN model. Several performance evaluation parameters have also been determined, which are not limited to root mean squared error (RMSE), and mean absolute error (MAE) but also include correlation coefficient (R), and coefficient of determination (R^2). Feature importance analysis is used to establish the influence of various features, and the model's variation is determined through a sensitivity analysis of the most important features. Moreover, other in-practiced machine learning techniques such as multilinear regression, Gaussian process regression, support vector machine, gene expression programming, and ensemble tree. Furthermore, lab-scale testing was carried out to validate the performance and results of our model. Finally, a graphical user interface (GUI) has been designed to make the suggested model easier to use.

2.3 Objectives

To close the research gap, the following research objectives have been established:

- Using Genetic Algorithms (GA), and Artificial Neural Networks (ANN) create a unique predictive model for compressive strength of High Early Strength Concrete (HESC) (GA)
- To compare the outcomes of the ANN-GA hybrid model with those of other in-practiced machine learning models
- The developed hybrid model validation through lab-scale testing

2.4 Structure of Report

There are six chapters in this thesis.

- **Chapter, 1; Introduction:** The introduction is the first chapter of this study, and it contains a broad introduction to concrete along with high early strength concrete.
- **Chapter, 2; Literature Review:** The literature study in Chapter 2 covers a thorough examination of applications of artificial intelligence tools in the field of civil engineering, particularly focusing on high-performance concrete. Moreover, this chapter also contains the objectives of this study.
- **Chapter, 3; Modelling Methods:** The third chapter examines modeling methods in-depth while giving particular attention to our utilized optimization and regression methods.
- **Chapter, 4; Methodology**: The full schematic followed along with the methods of this study are described in Chapter 4.
- **Chapter, 5; Results and Discussion:** The outcomes are presented and discussed in Chapter 5. Conclusions and future proposals are presented in the final chapter.

Chapter 3

DATA-DRIVEN MODELS

3.1 Neural Networks (NN)

3.1.1 General

Neural networks often famous as artificial neural networks are a family of machine learning technology that uses layers in a closed network to interpret data. The name of these networks originated from their similarity to the brains of humans. These aren't an ideal duplicate of brain processing, but they do mirror how neurons in the human mind work. For instance, the brain consists of the composition of interlinked neurons that receive information through dendrites. As shown in Figure 5, the neuron by the axon receives signals and distributes them to nearby neurons through terminals. While interconnected decision functions and layers compose artificial neural networks via axon-like edges and communicate with one another [45].

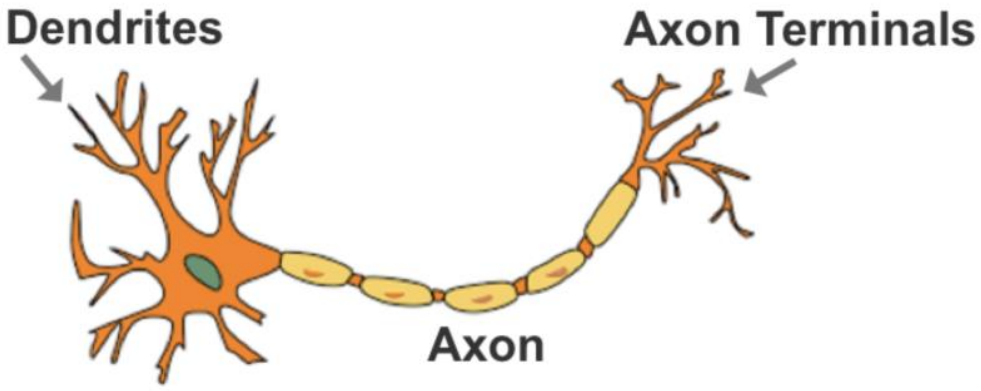

Figure 5 Structure of a Neuron in the Human Brain

3.1.2 Artificial Neural Network Types

In the domain of artificial intelligence, artificial neural networks (ANN) are among the most popular and widely used data processing approaches. These methods are easy to use and provide good performance at a minimal computing cost. the two most common forms of ANNs consists of single-layer networks (SLN) and multi-layer networks (MLN). SLNs are simpler to use and compute, whereas MLNs are better at addressing non-linear problems. They've been

used in a wide variety of engineering projects. MLNNs can be applied to a variety of regression situations [46]. The MLNN has input, output, and hidden layers, as depicted in Figure 6.

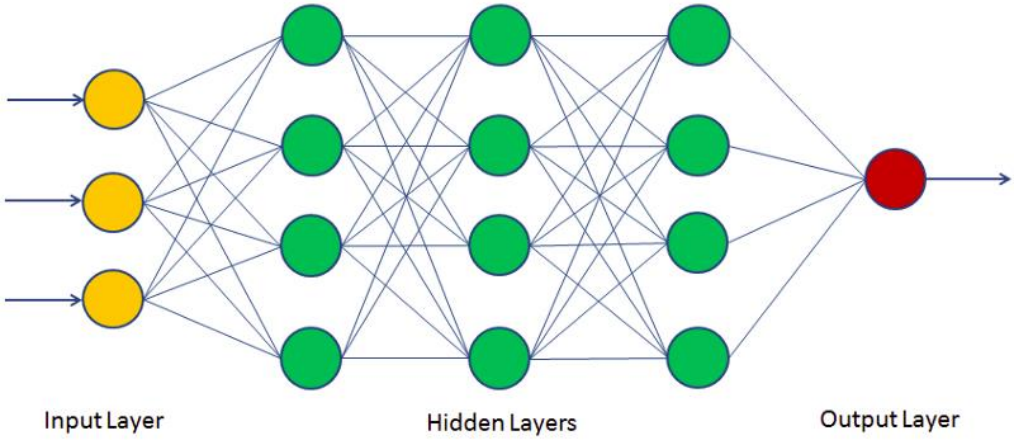

Figure 6 Different Layers of ANN

Multiple neurons are connected in a layer by weights in a sequential fashion. In the feed-forward stage, the network's output is predicted. Neurons convey data from the input set to the input layer, which is then sent to the hidden layer and finally to the output layer's neurons. This output is the model's forecast, which is derived using hidden and output layer calculations. Figure 7 depicts the process in one neuron. It is demonstrated that the inputs and their associated weights are used to construct the initial weighted sum of input data. To alter the output, which is generally a constant number, a biased value is additionally added. The weighted sum is calculated by

$$y=(x_1\times w_1)+(x_2\times w_2)+(x_3\times w_3)+b \quad [1]$$

where x_1, x_2, and x_3 denotes signals from input layers, and w_1, w_2, and w_3, respectively, are matching weights. In this equation, b is the biased value. Figure 7 shows how the node's summed weighted input is converted to an output that is delivered to the succeeding hidden layer. Moreover, activation functions are used to perform this task. The pure linear was utilized in the output layer whereas hyperbolic tangent sigmoid activation functions was utilized in the hidden layer, respectively which are commonly famous due to their robustness [47]. The transfer function equations are presented by

$$f_1 = \text{tansig}(t) = \left(\frac{2}{1+e^{-2t}}\right) - 1 \quad [2]$$

$$f_2 = \text{lin}(t) = t \quad [3]$$

The optimization techniques are then used to optimize the weights and biases. The change of weights and biases is repeated in this stage to decrease the prediction error. Resilient Backpropagation (RB), Conjugate Gradient (CG), Gradient Descent with Momentum (GDM), Levenberg-Marquardt (LM), and Gradient Descent (GD) are some of the most famous optimization methods utilized in ANN (LM) [48]. The Levenberg-Marquardt (LM) technique is a well-known and successful conventional optimization procedure that was applied in this study. After a defined number of generations, it intersects on the best vector of biases and initial weights [2, 46].

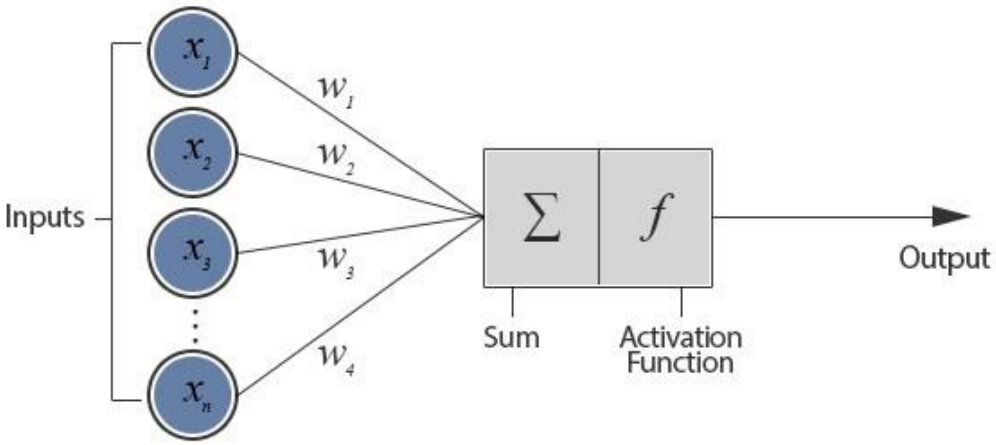

Figure 7 Processing of a Neuron in Artificial Network Structure

3.2 Evolutionary Optimization Method

3.2.1 Genetic Algorithm

A Genetic Algorithm (GA) is utilized in this work to choose the best ANN network. In 1975, J.H. Holland proposed the genetic algorithm initially and it is considered to be one of the efficient and most widely used algorithms that have a biological evolutionary basis. The underlying idea of GA is Darwin's hypothesis of survivance of the fittest [49]. The chromosome description consisting of genes, measurement of fitness values, and biological evolution through operators are thought of as key functions in the process of genetic algorithm. Figure 8 represents the GA workflow in its entirety. Many scholars have utilized GAs to analyze complex mix design optimization solutions [50, 51]. GA starts by generating a set of potential solutions, which are then compared to the objective function. To evolve successive generations, selection, crossover, and mutation operators are used. The chromosomes are chosen in the selection stage based on fitness values, whereas children are formed in the crossover step by randomly changing sequences. Finally, the bits of the chromosome are flipped at random using a probability value. This newly evolved population repeats the process until the required criteria are met [52].

When compared to traditional optimization methods, genetic algorithms have numerous advantages. The ability to deal with complexity and operate in parallel is the most impressive of these. These algorithms can handle a variety of fitness functions, which are not limited to stationary, continuous, linear, and random, but also include nonlinear, and dynamic fitness functions. Because each individual operates separately, the variables in the algorithm solution can investigate in different directions. This property makes it ideal for parallelizing algorithms in preparation for employment. It has the ability to change a variety of factors as well as groups of programmed chains.

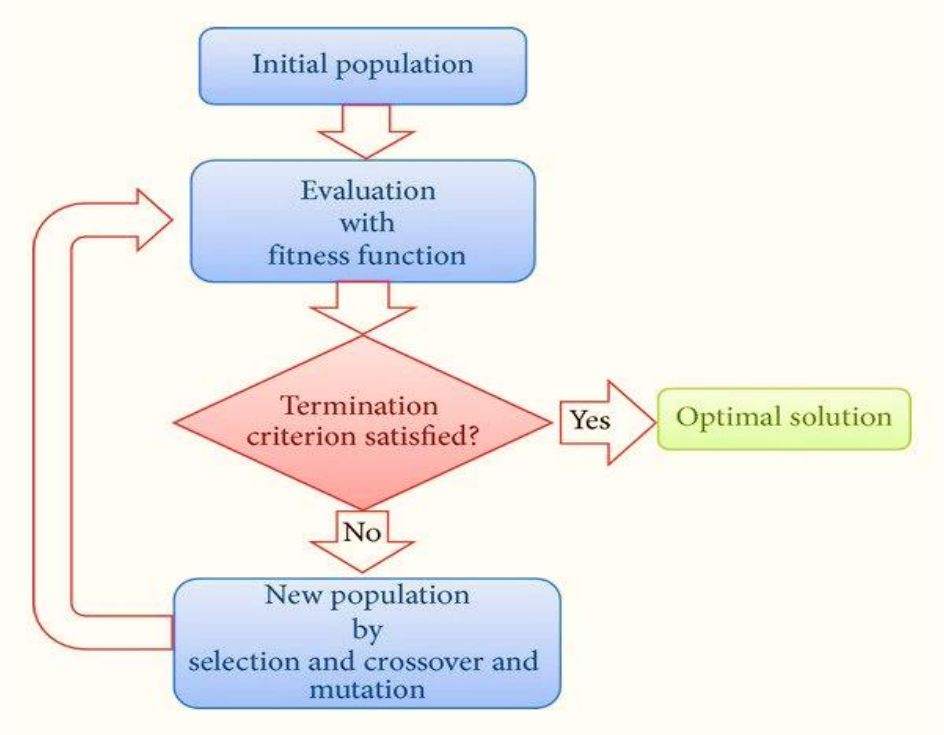

Figure 8 Process followed in GA

3.2.2 Parameters of GA

(a) Search Space or Primary Population

The encoding scheme (i.e., the process of encoding data into a specific format) is crucial in most computer tasks. The information provided is coded using a specific bit string. Several encoding methodologies are utilized depending on the issue domain: value-based, binary, permutation, hexadecimal, tree, and octal are all well-known encoding techniques [36]. Binary encoding is the most widely used strategy for encoding. One and zero strings are used to display every gene in a chromosome. Each bit in binary encoding represents a property of the answer. It speeds up the creation of crossover and mutation operators [52].

(b) Selection of best chromosome

Selection is also a vital phase in GA since it controls whether or not a string will be employed in the further reproduction. The selecting procedure is commonly called reproduction operation. The selection pressure determines the rate of convergence of GA. The most well-known selection procedures are not limited to tournament, roulette wheel, and Boltzmann, but also incorporate rank, and stochastic universal sampling [52]. The tournament selection is used

in this study which was first developed by Brindle (1983). Based on their fitness scores, the top individuals were selected from the roulette wheel. Following selection, individuals with higher fitness values are introduced to the following generation's pool. In this process of selection, everyone is compared to everyone else till the specified maximum value of the population is reached [36, 52]. Figure 9 demonstrated the tournament selection procedure.

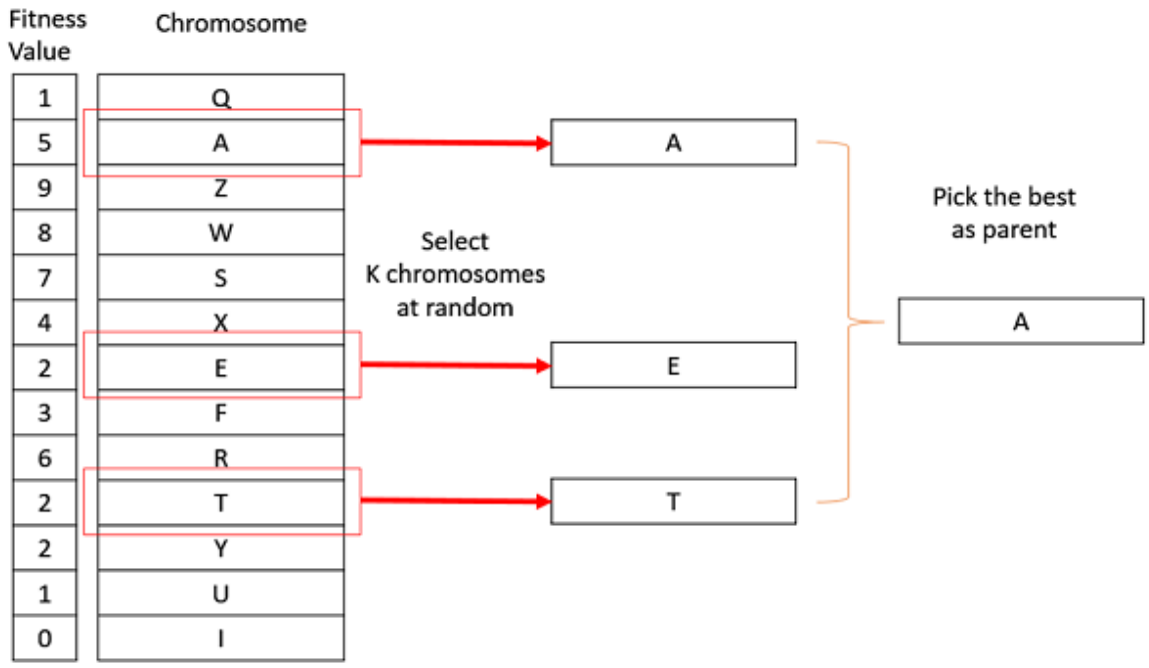

Figure 9 Best Chromosome Selection Thorough Tournament

(c) Crossover Techniques

To create new children, the genetic information of two or more parents is combined. Single-point crossover, uniform crossover, cycles crossover, shuffle crossover, k-point crossover, partially matched, and the reduced surrogate is all well-known crossover types [52]. In this study, a single-point crossover is used. The method followed by a single point is that first an arbitrary crossing point is chosen, and the chromosomes are exchanged at that point. Figure 10 shows the changed information of genes after it has been switched in one place. The one chromosome tail gets swapped by the head to make new children in this example.

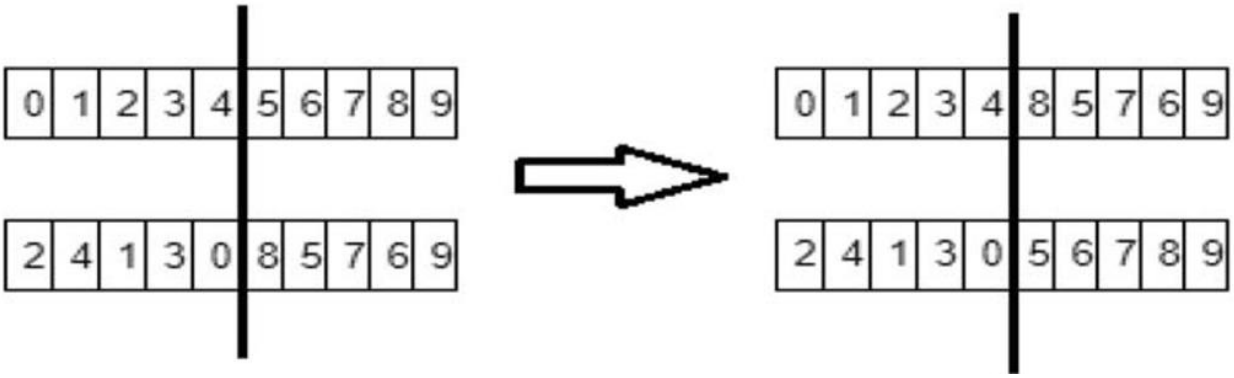

Figure 10 Swapping of Genetic Information after Single Point Crossover

(d) Techniques of Mutation

Mutation is a process that ensures that genetic variety is maintained from one generation to the next. Simple inversion, displacement, and scramble mutation are three popular mutation operators. The DM mutation moves a component of a string within a single solution. In addition to random displacement mutation, the place for displacement is picked at random from the supplied substring which causes a perfect solution. Two DM variations include insertion mutation and exchange mutation. In insertion and exchange mutations, a segment of the individual is either moved to a different site or swapped with other portions [36]. The mutation working for a single chromosome is illustrated in Figure 11**.**

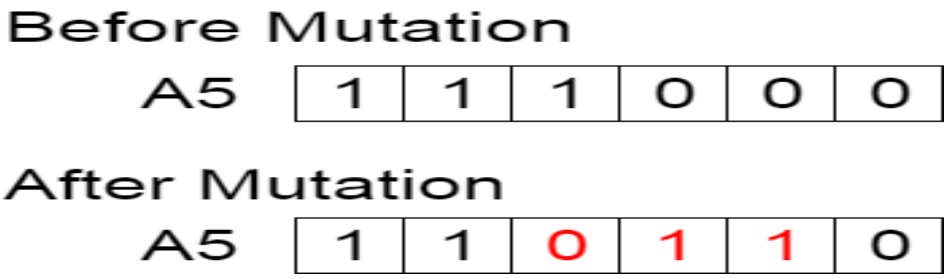

Figure 11 Change in Genes after Mutation Process

(e) Criteria of Stoppage for GA

Duration restriction, fitness limit, number of generations, number of stall generation, and stall time limit are just a few of the stopping criteria that can be utilized to end the GA. The

maximum number of generations is used as the halting criteria in this investigation. GA's pseudo-code is depicted in Figure 12. The genetic algorithm iterates as many times as possible until the global optimum solution is found, as seen in this pseudocode.

Input:
Population Size, n
Maximum number of iterations, MAX
Output:
Global best solution, Y_{bt}

begin
Generate initial population of n chromosomes $Y_i \ (i = 1, 2, ..., n)$
Set iteration counter $t = 0$
Compute the fitness value of each chromosomes
while $(t < MAX)$
Select a pair of chromosomes from initial population based on fitness
Apply crossover operation on selected pair with crossover probability
Apply mutation on the offspring with mutation probability
Replace old population with newly generated population
Increment the current iteration t by 1.
end while
return the best solution, Y_{bt}
end

Figure 12 GA Pseudocode [52]

3.3 Additional Methods in Machine Learning

3.3.1 Multi-Linear Regression

An approach for establishing the linear type of relationship among parameters and outputs is commonly known as linear regression which is statistical in nature. When there is just one input variable, simple linear regression is employed; when there are numerous input features, multiple linear regression is utilized (MLR).

$$y = \beta_0 + \beta_1 x_1 + \beta_2 x_2 + \cdots + \beta_n x_n \quad [4]$$

The number of input variables is specified by x_i (i = 1, 2...n), the term indicates the equation's coefficient, and y represents the model's output. The main purpose of MLR is to identify the best coefficient value [38].

3.3.2 Gene Expression Programming

Ferreira et al. [40] were the first who put forward the theory of a novel type of genetic programming widely known as Gene expression programming (GEP). The basic technique starts with the chromosomes that were randomly generated in the initial population. Afterwards, the chromosomes are revealed, and magnitude of fitness for each individual is calculated using criteria specified. After that, the change in fitness is established for all the chromosomes. Fitness-oriented individuals are passed down to the next generation. This procedure is repeated until the desired outcomes are achieved [41]. GEP has demonstrated good accuracy in predicting the compressive strength of geopolymer concrete, waste sand foundry concrete, high-performance concrete, and recycled concrete types as compared to other models [53, 54]. Gepsoft XProTools, which features the interface seen in Figure 13, uses GEP.

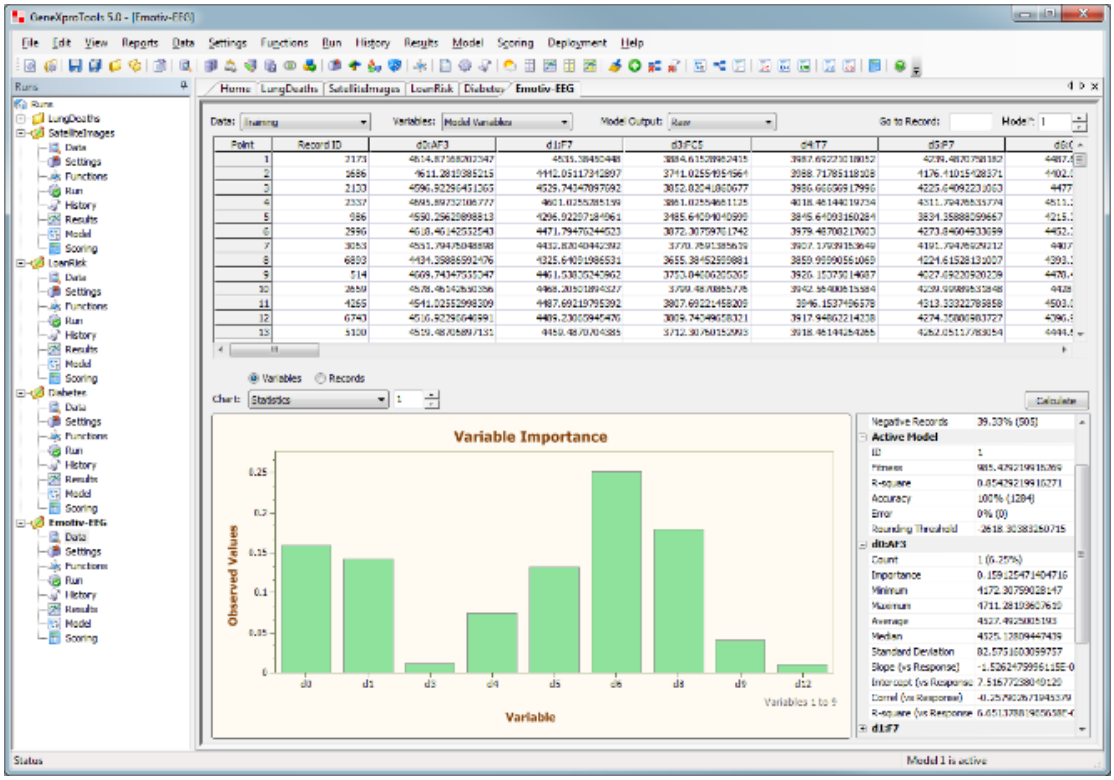

Figure 13 Classical Interface of GepSoft Xpro Tools

For the GEP model, the following parameters were chosen. The prediction procedure in GEP involves numerous iterations. The results of an analysis are checked every time when it is performed and compared. Variables such as the linking function, tail size, head size, and chromosomes amount will be altered in the next iteration until the program reaches to an optimum value of solution. Table 1 shows the optimal parameter settings. The optimal genes determined was three (3), tail size was eleven (11) and head size was (10) along with chromosome value of eighty (80). In addition, to avoid overfitting the solution, the function for linkage employed in this investigation was addition (+), and no changes are made in the rest of variables.

Table 1 Important Parameter Values used in GEP Program

General Settings	
Linking Function:	Addition
Fitness Function:	MAE
Genes:	3
Gene Size:	70
Chromosomes:	80
Dc Size:	11
Tail Size:	11
Head Size:	10
Genetic operators	
Rate of Mutation:	0.00137
Rate of Inversion:	0.00546
Rate of Gene Transposition:	0.00277
Rate of Gene Recombination:	0.00277
Rate of Recombination:	0.00277
Rate of Transposition:	0.00546
Numerical	
Per Gene:	12
Type of Data:	Floating number
Bound lower:	-12
Bound Upper:	12

3.3.5 Ensemble of Decision Trees

An ensemble of the tree (ET) is a type of decision tree graph for making decisions that looks like a tree. Regression and classification trees are two different forms of ensemble trees that produce numeric and categorical values in output, respectively. The approach of the ensemble of regression consists of numerous regression trees combined in a weighted combination, which is subsequently used for predictive modeling. An ensemble tree's prediction performance is improved by combining many regression trees. These are most suitable due to their speed and comparative stability in complex problems. As a result, it is frequently possible to achieve synergy among different types of trees in a numerical problem. A typical method for enhancing diversity in the prediction of ensemble trees is to utilize trees that select features based on the random distribution of data. Figure 14 depicts a simple decision tree that can be used for regression.

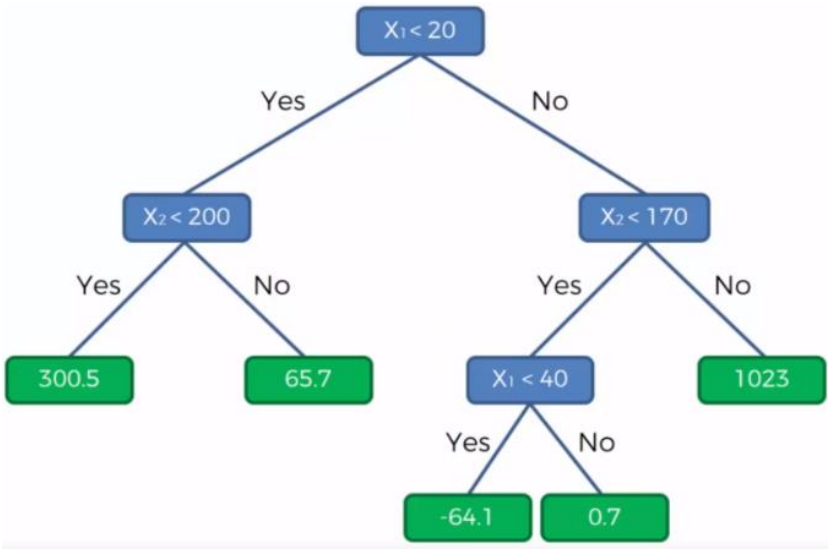

Figure 14 Simple Illustration of Ensemble Tree

3.3.2 Support Vector Machine

Support vector machines are supervised machine learning models that are commonly used to solve regression and classification issues. In both classification and regression tasks, the SVM uses the kernel function to create the correspondence between input and output data. In complex circumstances including dynamic nonlinearity, the kernel function is quite useful. Inseparable variables are translated into high dimensionality, which is impossible to achieve in lesser dimensionality [38]. Because of its high robustness, the cubic kernel function was utilized in this investigation. The typical form of support vector algorithm is depicted in Figure 15. A hyperplane is employed to distinguish between two groups of solutions in this diagram. Two types of support vectors are depicted by the blue and green points.

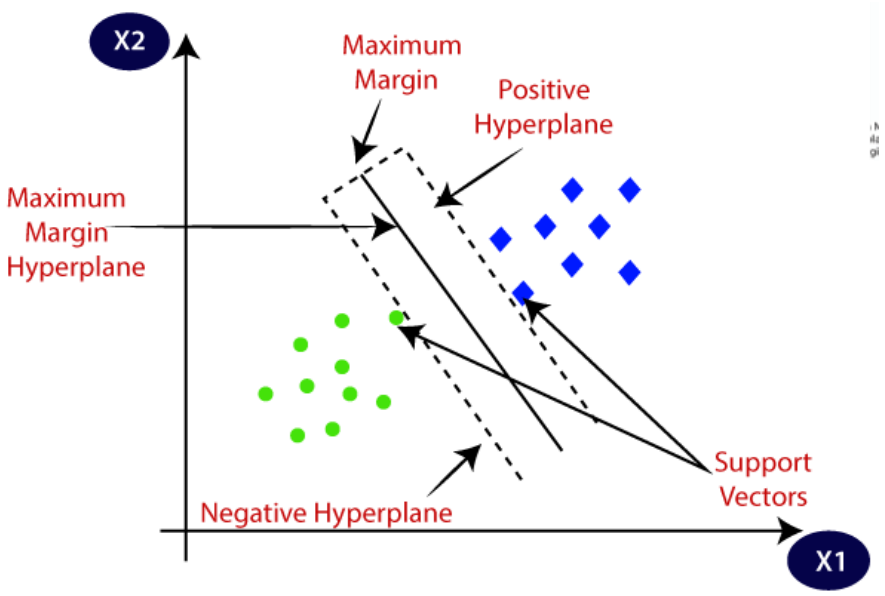

Figure 15 Support Vectors and Planes used in SVM

3.3.3 Gaussian Process Regression

The Gaussian process is a set of variables that produce a Gaussian distribution. It's also commonly utilized to solve regression issues which are also famous as a distributional function because it consists of average function m (y) and function of covariance k (y,y′). The average function m (y), which indicates the value of function on value of x specified by Equation (5). It is the mean of functions calculated in the given range of x.The covariance function k (y,y′) is defined by Eq (6), and it illustrates the relationship for each input pair (y,y′) function value. Consequently, Equation (5) demonstrated a GP, while Equation (6) denotes a function (7) [39].

$$m\,(y) = E[f\,(y)] \tag{5}$$

$$k\left(y, y^{'}\right) = E\left[\left(f\,(y) - m(y)\right)\left(f\left(y^{'}\right) - m\left(y^{'}\right)\right)\right] \tag{6}$$

$$f\,(y) \sim GP\left(m(y), k\left(y, y^{'}\right)\right) \tag{7}$$

The kernel function must be properly designed to produce an effective GP regression model. As previously stated, the kernel function quantifies the dependencies between output values and their input values. In other words, the values of inputs reflects the expected output values' similarity. The distance between input values is frequently used to represent similarity in this situation. Figure 16 displays a gaussian process for prediction, with the blue line representing

the GPR function and the dots representing the datapoints. There are various distinct kernel functions described in the literature, including the rational quadratic, squared exponential, non-iso tropic mattern class of kernels, and many others [39]. The kernel function employed in the development of the model after much research is non-isotropic Mattern.

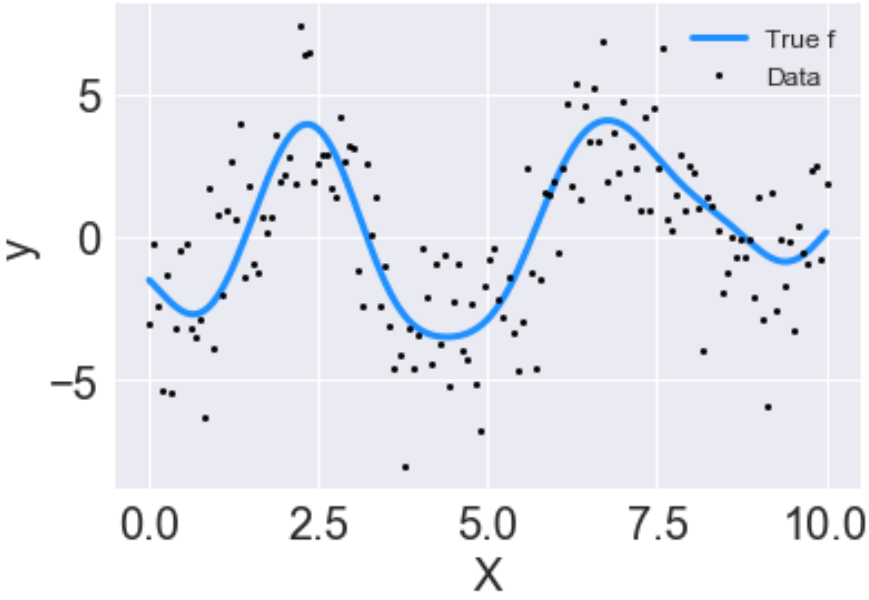

Figure 16 Predictive Modelling using GPR Model

Chapter 4

RESEARCH METHODOLOGY

4.1 Overall Scheme

Figure 17 depicts the general flowchart used in this study, which is divided into three phases and each phase is equally important for the proposed study. Phase-1 consists of data handling, whereas phase-2 comprises model development, and in phase-3 validation of the proposed model is performed. Phase 1 consists of data handling in which first data collection from literature is done and after that data importing into MATLAB was done. Data preprocessing was performed before the Artificial Neural Network (ANN) Model Development in Phase-2. In this phase, first ANN optimal Architecture is selected through GA which is then used in ANN Model Development. To evaluate the model behavior feature Importance and partial dependence plots are plotted. In the final Phase-3, Model Validation is done using comparison with other Machine Learning Models along with Experimental Verification and development of Graphical User Interface (GUI).

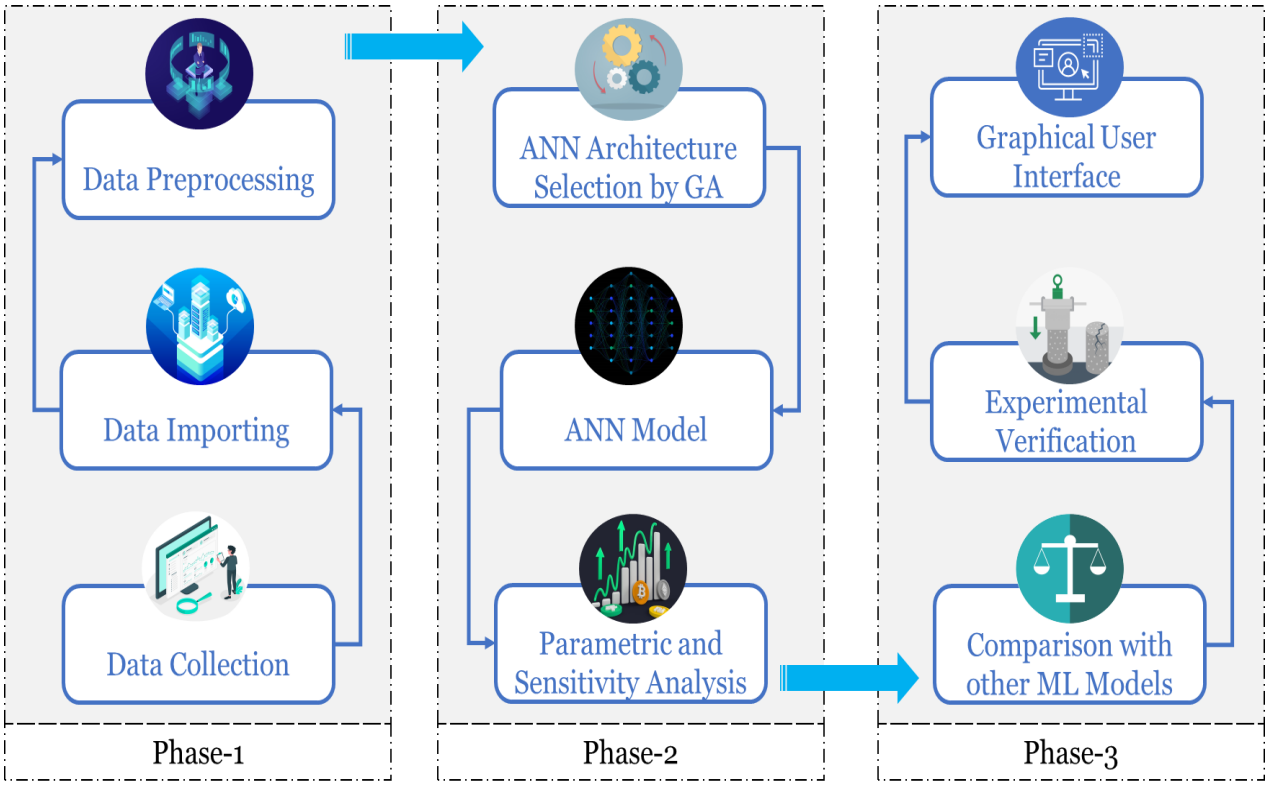

Figure 17 Proposed Workflow of this Study

4.2 Pre-Processing along with Data Collection

Using various keywords (early strength development, rapid hardening concrete, high early strength concrete, compressive strength), a detailed literature review was conducted to obtain lab results of experiments on the compressive strength of HESC. Google Scholar and Science Direct were used to search for published papers. From 39 internationally published studies, 869 experimental results values comprising cylinders and cubes testing were compiled for the compressive strength of HESC [4, 5, 7, 8, 10-20, 24, 55-72]. Eleven input variables were chosen based on the availability of data and their impact on HESC compressive strength. There were eight numerical variables and three category variables in this study. Dataset compilation was the core basis for further model design and development, as demonstrated in the schematic phases of this study in Figure 17. Table 2 shows the results of the statistical analysis of the obtained databases.

Table 2 Important Statistical Parameters for Data Collected

Variable	Full-Form	Unit	Type	Minimum	Maximum	SD
Age	Age	days	numerical	1	28	10.56
C	Cement	kg/m3	numerical	80	863.2	167.23
CA	Coarse Aggregate	kg/m3	numerical	0	2120	413.58
FA	Fine Aggregate	kg/m3	numerical	0	1712	271.85
MA-1	Mineral Admixture-1	kg/m3	numerical	0	380.93	99.78
MA-2	Mineral Admixture-2	kg/m3	numerical	0	200	29.97
SP	Super-plasticizer	kg/m3	numerical	0	21.6	6.99
W/B	Water-Binder	-	numerical	0.18	0.75	0.12
C_Type	Types of Cement	-	categorical	CSA	CEM I 42.5 N	-
MA-1_Type	Mineral Admixture-1 Type	-	categorical	PIA	FAF	-
MA-2_Type	Mineral Admixture-2 Type	-	categorical	BEP	NULL	-

The variables chosen for the model development based on the compressive strength influence include cement type (C) and quantity, mineral admixture-1 type (MA-1) and quantity, mineral admixture-2 (MA-2) type, and quantity. MA-2 mostly comprises different types of nanomaterials that are used nowadays in the enhancement of concrete properties especially fresh and early age characteristics. In addition, amounts of coarse (CA) and fine aggregate (FA) are also selected along with water to binder ratio (W/B) to check their impact on the HESC strength. It is also noted that compressive strength is a factor in the specimen curing period which made it necessary to include the age of the concrete. In this study, the collected data varies from 1-day to 28-days of testing for both cylinders and cubes. To address outliers and missing data points, the acquired data were preprocessed, and statistical analysis was performed before model building. The histograms of various input variables are displayed in Figure 18, while pie charts of categorical variables are demonstrated in Figure 19.

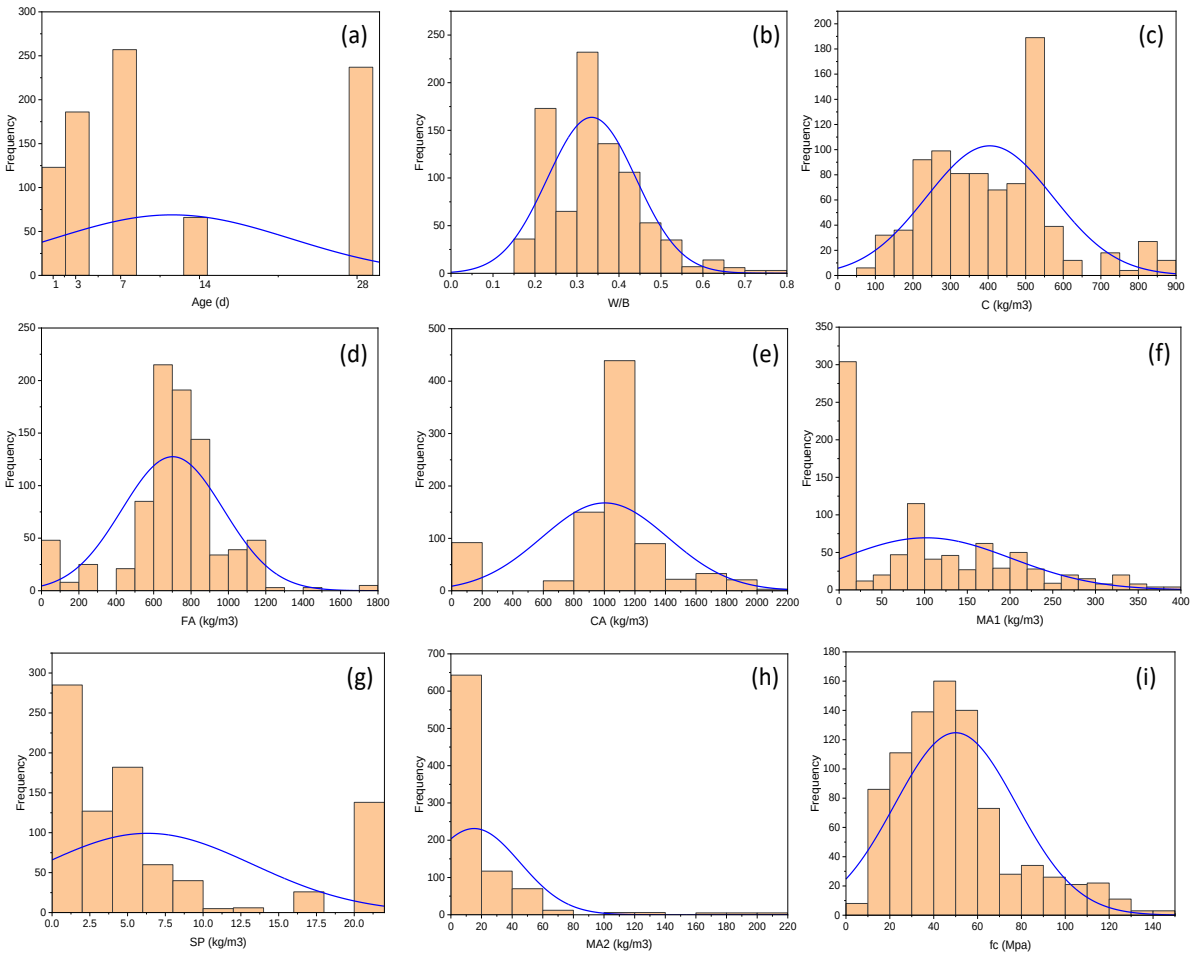

Figure 18 Historical Distribution of (a) Age, (b) W/B, (c) C, (d) FA, (e) CA, (f) MA-1, (g) SP, (h) MA-2, (i) f_c

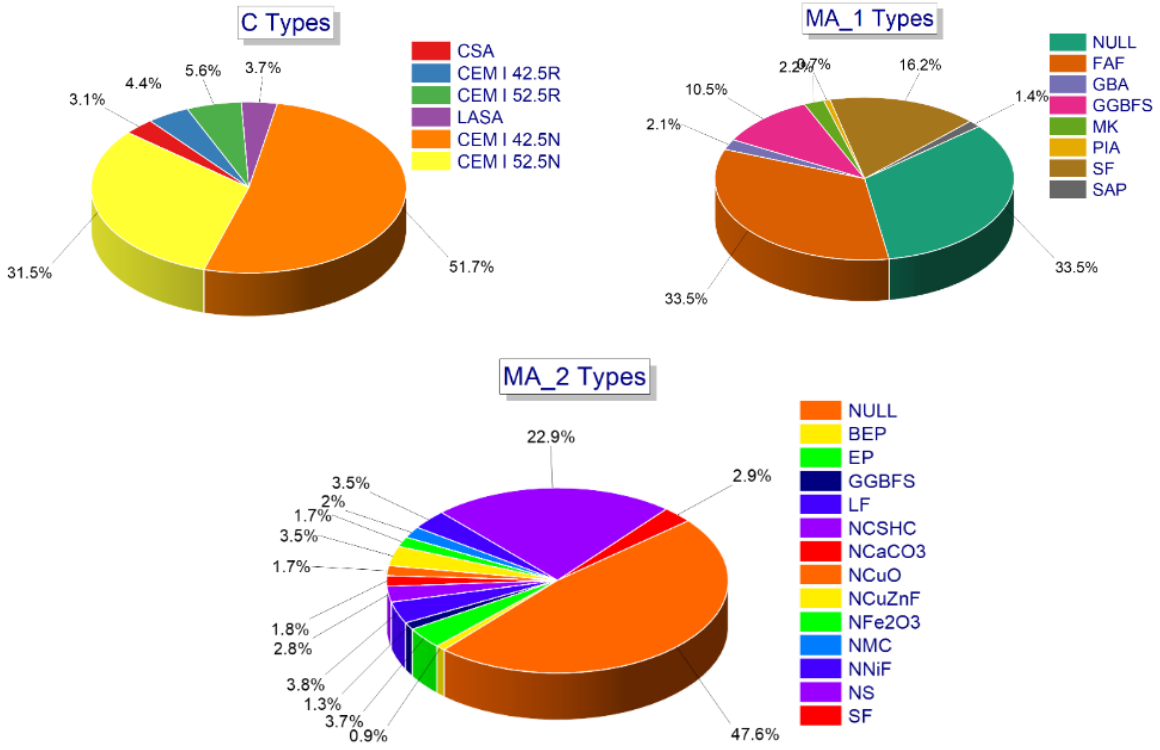

Figure 19 Categorical Distribution of (a) Cement Types, (b) Mineral Admixture-1 Types, (c) Mineral Admixture-2 Types

4.3 Experimentation of HESC

Experiments in the lab have been carried out to further validate our model. Two cement types and two mineral additive types were employed in this experiment. CEM I 42.5N and CEM I 52.5N types of cement are utilized, with N referring to typical early strength and meeting the regulatory standards [73]. Fly ash class F and silica fume are the two mineral admixtures used in this study. The chemical compositions of cement types and fly ash-F are shown in Table 3. Silica fume meet ASTM C1240 criteria whereas fly ash meet ASTM C618 criteria [74, 75].

Table 3 Oxide Composition for Fly Ash-F, CEM I 52.5N, and CEM I 42.5N

Chemical Composition	Fly Ash-F %	CEM I 52.5N %	CEM I 42.5N %
SiO_2	47.2	20.44	20.35
Al_2O_3	25.44	4.88	4.87
CaO	3.38	63.25	63.5
Fe_2O_3	2	3.4	3.26
MgO	1.4	2.24	2.41
SO_3	0.57	2.71	2.71
K_2O	-	0.57	0.58
NA_2O_3	-	0.07	-
Loss on Ignition	3.9	3.72	1.83
Chloride Content	-	0.01	-

Gravel and margalla sand were used as coarse and fine aggregates, respectively. To assess the aggregate characteristics, preliminary testing was undertaken on the aggregates before the formation of the mixture. These features help determine the appropriate mix proportion for the desired strength. The tests include water absorption, fineness modulus, gradation test, and specific gravity. The physical parameters of the raw material are listed in Table 4 and are in accordance with ASTM standards [76, 77]. To obtain good workability, a poly carboxylic-based super-plasticizer was utilized, and water from the tap was used for mixing.

Table 4 Summary of Properties for Fine Aggregate, Coarse Aggregate, and Silica Fume

Material	Specific Gravity	Fineness Modulus	Absorption
Silica Fume	2.24	-	-
Coarse Aggregate	2.65	2.55	0.73
Fine Aggregate	2.68	2.89	2.16

The volumetric approach is used to proportion the concrete mixture. The range of water to binder was from 0.23 to 0.32 by weight for the proposed mixtures and the ACI mix design method was used to create four recipes [78]. The mixed design of recipes is shown in Table 5. Mixes are made with cylindrical specimens measuring 100 mm x 200 mm. ASTM C 192 is used to make the mixtures. The dry mixing of aggregates is done by hand first, then the cement and mineral additives are added. The pan mixer was used to do the wet mixing after the dry mixing. The superplasticizer was applied during the wet mixing process according to ASTM specifications. The cylinders were cleaned and oiled before being filled with concrete. Concrete is poured in three layers, and examples are tamped using a mechanical vibrator. After one day of air curing, the concrete samples are demolded and placed in lime water for the requisite testing duration. To avoid any variations in strength due to surface roughness, specimens are properly caped prior to testing. Figure 20 depicts concrete samples after they have been poured, whereas Figure 21 depicts the concrete casting and testing procedure.

Table 5 Proportions of Mixtures per Cubic Meter of HESC

Mix ID	**I-1**	**I-2**	**I-3**	**I-4**
Cement Type	CEM I 42.5N	CEM I 52.5N	CEM I 52.5N	CEM I 52.5N
Mineral Admixture-1 Type	Fly Ash-F	Fly Ash-F	Silica Fume	Fly Ash-F
Mineral Admixture-2 Type	NULL	NULL	NULL	Silica Fume
Cement	400	400	320	500
Coarse Aggregate	842	842	674	851
Fine Aggregate	551	551	446	602
Mineral Admixture-1	80	80	48	80
Mineral Admixture-2	0	0	0	42
Superplasticizer	2.0	2.0	12.7	5.6
Water-Binder Ratio	0.28	0.28	0.25	0.24

Figure 20 Samples for Compressive Strength

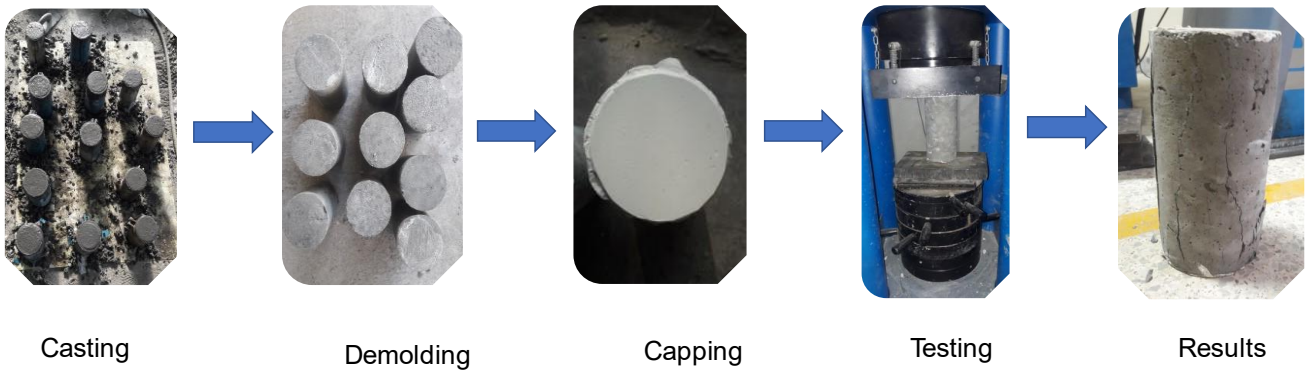

Figure 21 Schematic Flow of Testing from Casting to Final Results

Chapter 5

RESULTS WITH DISCUSSION

5.1 Developed Framework for the Model

This study proposes an integrated model of Artificial Neural Networks and Genetic Algorithms. The most common way for choosing an ANN design is hit and trial [46, 79]. This is a difficult task that wastes a lot of time and may also result in the model underfitting or overfitting [80]. A genetic algorithm (GA), which presents an evolutionary technique to handle such challenges, is the most robust approach for the optimal architecture of ANN. As a result, in this research, GA is employed to determine the best layers and their associated neurons for ANN.

For model development, the MATLAB R2021b is employed. The data is divided into 3 datasets at random: training (seventy percent), validation (fifteen percent), and testing (fifteen percent). The model is trained using the training part while the testing portion is employed to evaluate its validity. When over-fitting occurs, the validation data is used to stop the training. The Levenberg-Marquardt technique was used to train the ANN model using the data acquired, and the multilayer neural network was trained with the feed-forward type of neural network. Whereas the model had only one output and errors were optimized using the backpropagation technique. The eleven variables were supplied into the model as inputs, and the model's output was compressive strength. To choose the optimal hidden layers and number of neurons of the population, the type of genetic algorithm approach used was single-objective which was set as the mean-squared error (MSE).

Figure 22 depicts the integrated approach's overall framework. The imported data is split into two groups. The training and validation part make up the first set, while testing data make up the second. Following that, a sample of the initial search space consisting of hidden layers and neurons is created and further evaluation is done on this initial population with the help of fitness function. Following that, GA operators are used to construct the following generations. This method is repeated until a certain number of generations has been reached. The ideal ANN design chosen by GA comprises two hidden layers, as seen in fig. As indicated in Figure 22, the amount of neurons in the first and second layers were nineteen (19) and twenty (20), respectively.

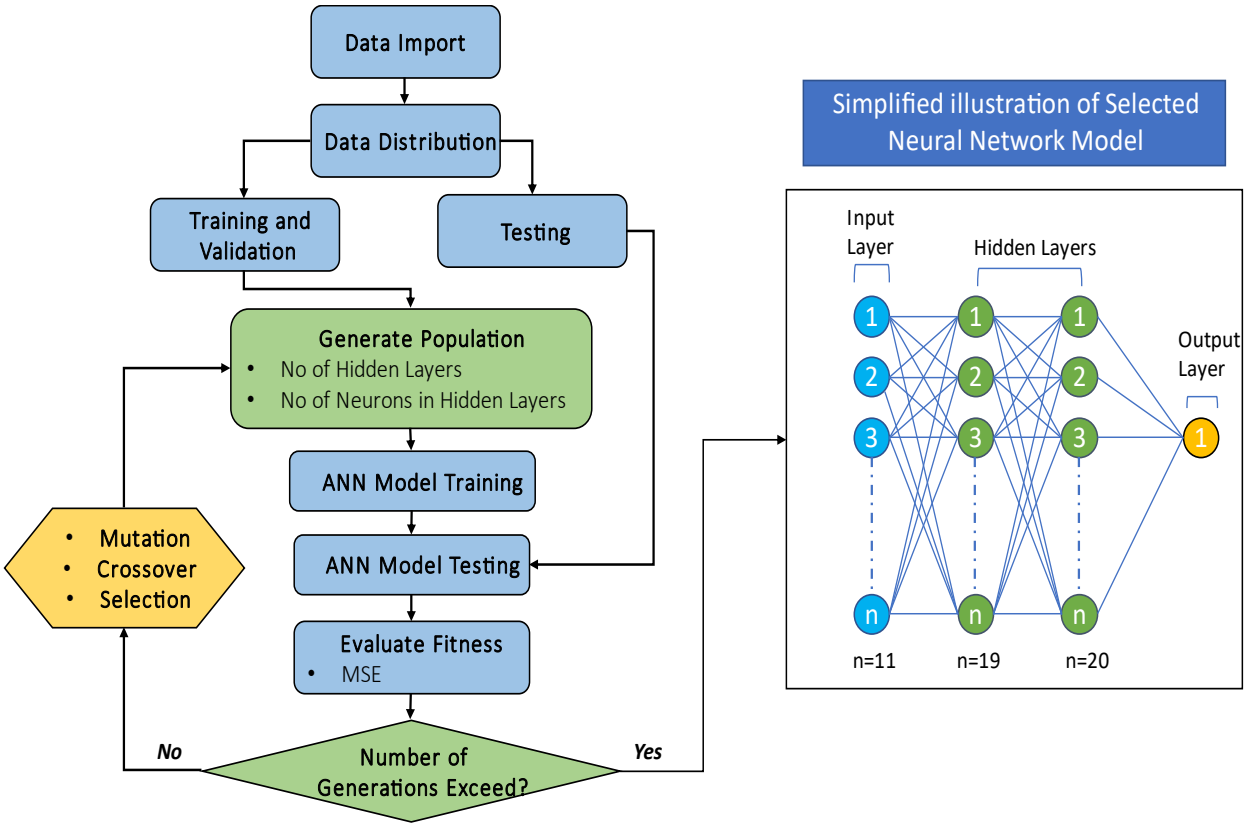

Figure 22 GA Selection of ANN Framework and Selected Optimal Architecture

5.2 Performance of Developed Hybrid System

The commonly used performance metric is the coefficient of correlation (R) in most of the previous studies, however, because of its sensitivity to multiplication and division function by a predetermined value, R cannot be utilized as the sole parameter for assessment of the model. As a result, the study calculates the coefficient of determination (R^2), root-mean-square error (RMSE), and mean absolute error (MAE). The model's performance will be evaluated using these parameters. The equations of performance parameters used are given below

$$R = \frac{\sum_i^n \left(x_i^e - x_{avg}^e\right)\left(x_i - x_i^{avg}\right)}{\sqrt{\sum_i^n \left(x_i^e - x_{avg}^e\right)^2 \sum_i^n \left(x_i - x_i^{avg}\right)}} \quad [8]$$

$$R^2 = 1 - \frac{\sum_i^n (x_i^e - x_i)^2}{\sum_i^n \left(x_i^e - x_{avg}^e\right)^2} \quad [9]$$

$$RMSE = \sqrt{\frac{1}{n}\sum_i^n (x_i^e - x_i)^2} \quad [10]$$

$$MAE = \sum_i^n |x_i^e - x_i| \quad [11]$$

Where, x_i= predicted value, x_i^e = experiment value, x_{avg}^e = average of experiment values, x_i^{avg} = average of predicted values.

The small circles in brown color in Figure 23 show the forecasted and experimental values for f_c in MPa obtained from the hybrid ANN model shown. The fit lines in the linear form for the training, validation, and testing data are shown in blue, green, and red, respectively. The discrepancy between predicted and experimental values is quite small for all datasets (training and testing), as shown in Figure 23**.** In addition, the overall R-graph shows that very a much smaller number of data points deviated from the linear fit line. A model with a coefficient of correlation (R) near one is considered good. Our overall R-value is 0.983, indicating that the model is performing well.

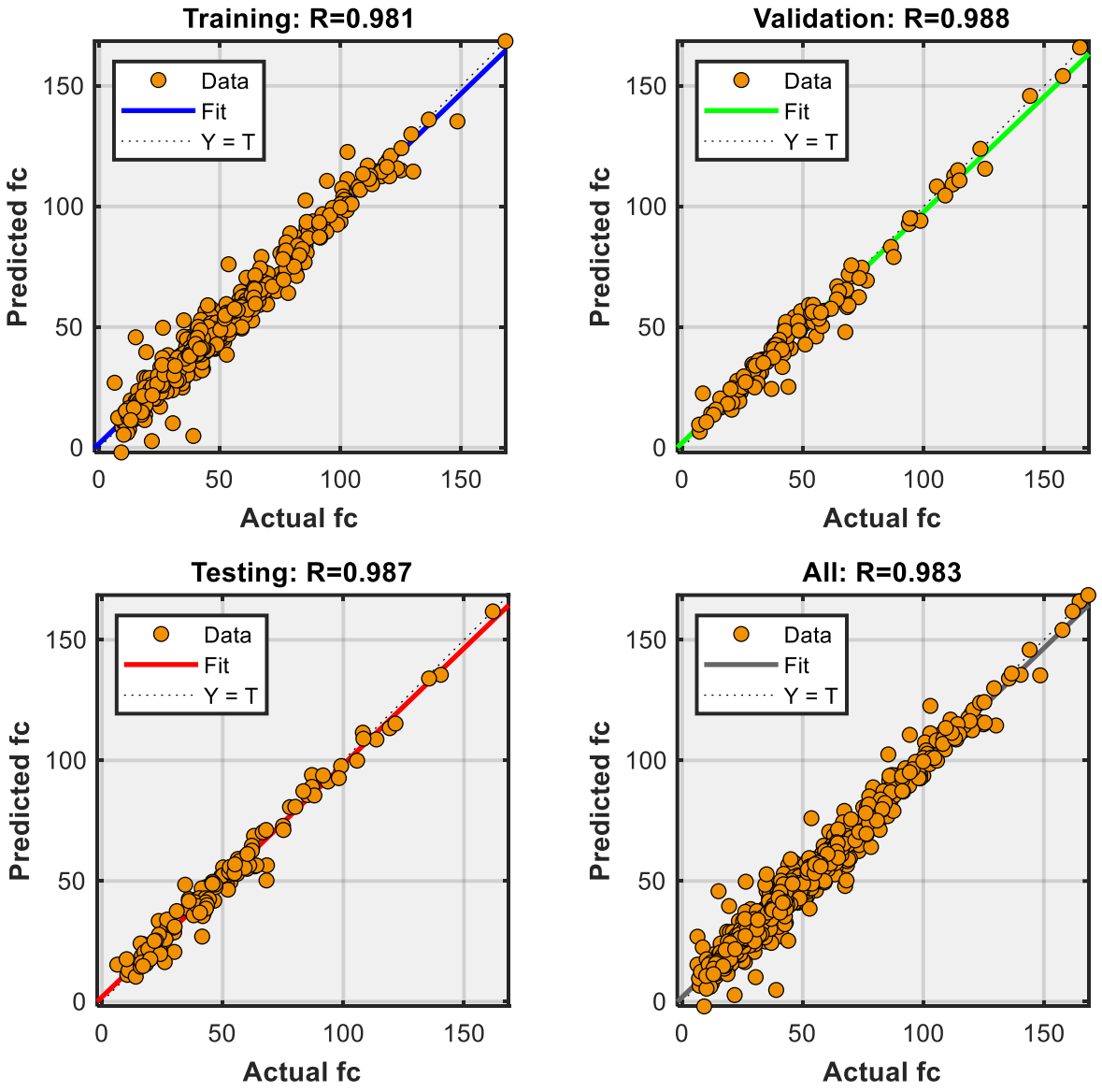

Figure 23 Performance of the Model with Regression Coefficients for different datasets

The performance matrices calculated for the developed model are listed in Table 6 which consists of MAE and RMSE along with correlation and determination coefficients for the testing and training stages. In the testing phase, the model shown a comparatively less error values (MAE = 3.14, RMSE = 4.06), as compared to training phase (MAE = 3.51, RMSE = 5.06). Similar performance was observed for the correlation and determination values which were higher in the testing phase (R = 0.987, R^2 = 0.975) and comparatively lower in training stage (R = 0.981, R^2 = 0.962) as shown in Table 6. The least mean absolute error value was noted as 3.14 while the greatest R for the testing set shown by modal was 0.987. The statistical measures in Table 6 reveal that the proposed model (Hybrid ANN-GA) performs well with an

efficient ability to predict the compressive strength of HESC at all ages including early (1,3 days) and final strength (28 days).

Table 6 Training and Testing Dataset Performance Indices

Statistic	Parameter	Testing	Training
Mean Absolute Error	MAE	3.14	3.513
Root Mean Square Error	RMSE	4.05	5.068
Coefficient of Correlation	R	0.987	0.981
Coefficient of Determination	R^2	0.975	0.962

The proposed model's error histogram is shown in Figure 24. It compares the optimized ANN-GA prediction model's error distribution, which is calculated by taking the difference between predicted and experimental values. The projected error of the developed hybrid ANN model demonstrated Gaussian distribution where the error lies evenly on both sides of peak values. The concentration of error noted was in the [-6, 6] area for all considered values. Figure 24 shows that the suggested hybrid model is robust and delivers accurate experimental value predictions.

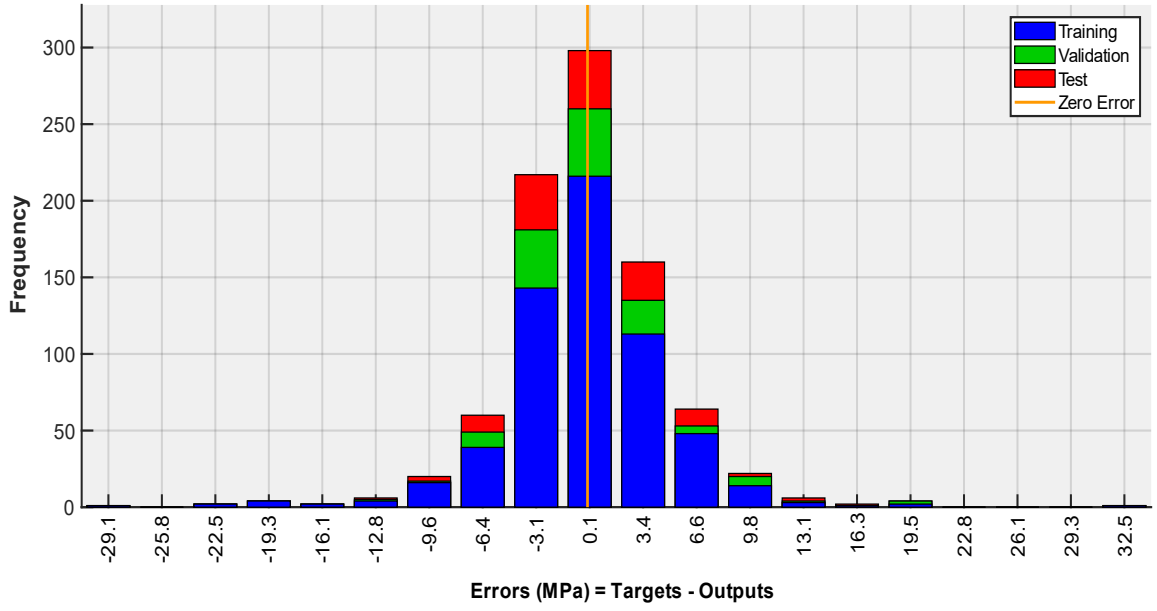

Figure 24 ANN Hybrid Model Error Distribution Showing Normal Distribution

5.3 Model Validation Through Other Machine Learning Techniques

MATLAB 2021b inbuilt programs were used to evaluate the performance of the ANN-GA model with various in-practiced machine learning techniques including support vector machine (SVM), and Gaussian process regression (GPR) along with ensemble tree (ET) and multi-linear regressions (MLR). In addition, a relatively new technique known as gene expression programming (GEP) used in several studies has also been employed in order to compare the performance. Table 7 shows the performance indices of the models under consideration.

The investigation shows that the other developed models are capable of predicting compressive strength at all phases, however, the performance regarding R and R^2 was highest for the hybrid ANN model among all. The ANN-GA model has the excellent coefficient values both in training (R = 0.981, R^2 = 0.962), and testing stages (R = 0.987, R^2= 0.975). The GPR model was the second best with an R-value of 0.954, and an R^2-value of 0.910 in the training and in testing these were 0.976 and 0.954 respectively. Furthermore, the SVM and ET models both performed well and had similar performance matrices in training, with R and R^2 values that were near to one other, but they differed slightly in testing. The remaining two models, MLR and GEP, produced acceptable outcomes but were less accurate than previous others, as evidenced by their R-values of 0.911, and 0.9 in training respectively. In addition, their fitness in the testing phase was 0.925 and 0.918, respectively also demonstrating their low predictability. The MLR model performs the worst in terms of determination coefficient values with a 0.83 value.

The assessment of the developed models has also been carried out for the error indices where low error values were an indication of superior performance. In both the training and testing stages, the hybrid ANN model beat all other models with a mean absolute error of 3.51, a root-mean-square error of 5.068 in the training stage, and a mean absolute error of 3.14, and a root-mean-square error of 4.05 in the training stage. Other models performed relatively low when compared with the ANN model, with MLR having the worst performance in both training (MAE = 8.60, RMSE = 11.97) and testing (MAE = 8.67, RMSE = 12.2). MLR's poor performance when compared to the remaining models is due to the non-linear connection of compressive strength with the variables.

To summarize, different machine learning models were built and tested for the compressive strength prediction of HESC, including MLR, RF, SVM, and ET. Most of the developed model's accuracy was good while considering the non-linearity of input parameters. The hybrid

ANN model demonstrated the highest efficiency for regression coefficients (R, R^2) as compared with others (SVM, ET, GPR, and GEP). When compared to the other models, the MLR model fared badly during both training and testing. For training the hierarchy of performance followed was ANN-GA > GPR > SVM = ET > GEP > MLR and for testing the pattern shown was ANN-GA > GPR > SVM > ET > GEP > MLR. At the end, the outcomes of the developed models were assessed in error terms also, which showed the same patterns. Thus, most of the developed models have good prediction accuracy, but the proposed model with hybridization (ANN-GA) surpasses remaining and may be employed to anticipate compressive strength while eliminating the requirement for tests in the labs whereby preserving resources and efficiency.

Table 7 Comparative Analysis of Performance Matrices for Different Developed Models

	R		**R^2**		**RMSE**		**MAE**	
Model	**Training**	**Testing**	**Training**	**Testing**	**Training**	**Testing**	**Training**	**Testing**
ANN-GA	**0.981**	**0.987**	**0.962**	**0.975**	**5.068**	**4.050**	**3.513**	**3.140**
GPR	0.954	0.976	0.910	0.954	8.103	6.301	5.499	4.519
SVM	0.927	0.955	0.860	0.907	10.378	8.960	7.500	6.960
ET	0.927	0.947	0.860	0.879	10.129	9.800	7.420	7.100
GEP	0.911	0.925	0.83	0.856	11.135	11.24	8.560	8.61
MLR	0.900	0.918	0.810	0.843	11.974	12.200	8.606	8.670

MLR = Multi Linear Regression, GEP = Gene Expression Programming, EN = Ensemble Tree, SVM = Support Vector Machine, GPR = Gaussian Process Regression, ANN-GA = Artificial Neural Network-Genetic Algorithm

5.3 Knowledge Extraction and Model Explainability

In the modern era of explainable machine learning, feature importance and sensitivity analysis are useful to deepen the knowledge of the model. Figure 25 depicts the proposed model's feature importance. As seen in Figure 25, practically all parameters contribute to HESC's compressive strength but the quantity of cement and the water-binder ratio were the top candidates. The amount of cement used is critical because an increase in cement quantity has been shown in earlier research to alter early and 28-day strength [44]. Along with these two variables, the concrete's age, W/B, and super-plasticizer all also have an impact on HESC's compressive strength, as these factors play a role in strength development. The kind of mineral admixture-2, which contains mostly nanomaterials, was found to be the least important parameter. The fact that the type of nanomaterial has a smaller impact on compressive strength than its quantity backs this up [22, 23].

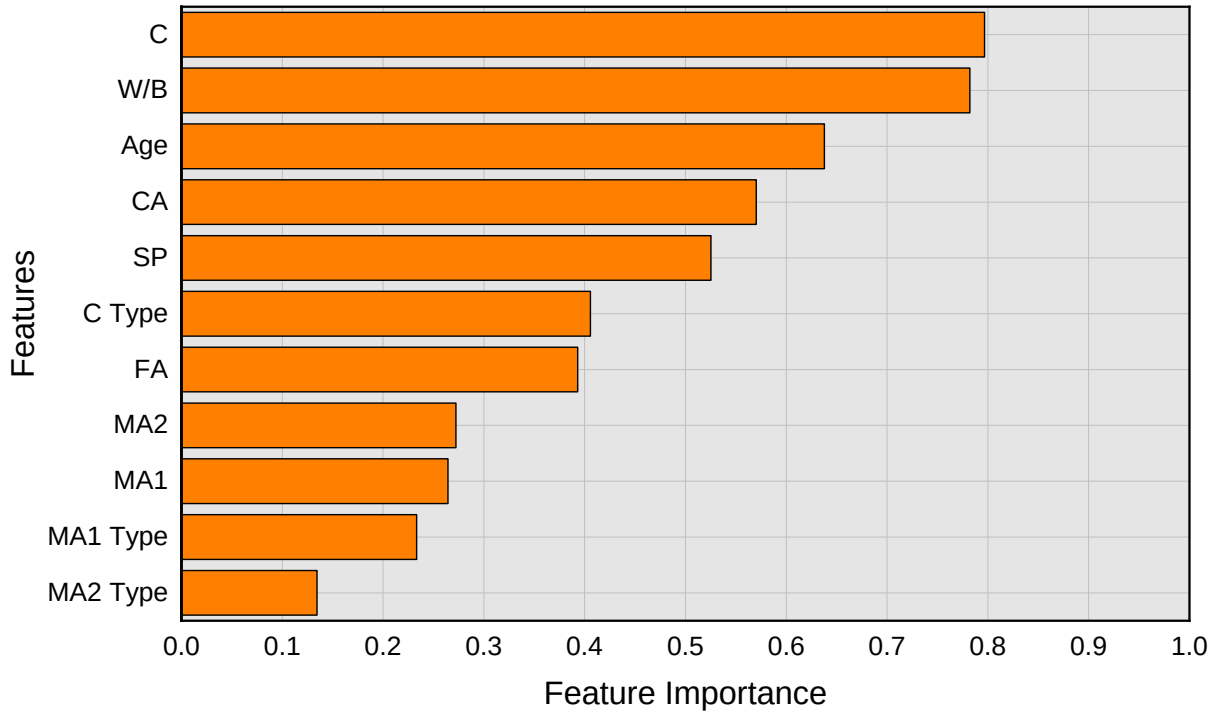

Figure 25 Relative Importance of Input Parameters on the Model

Partial dependence plot (PDP) analysis is being employed on the proposed hybrid ANN model to analyze the input parameters' influence on predictability. The compressive strength behavior of HESC is evaluated by utilizing the ANN model by changing one parameter in the suitable range while maintaining all others fixed [81]. Figure 26 depicts the PDP graphs of the five most critical input parameters.

PDP plots of the important influencing variables are shown in Figure 26 (a, b, c, d, and e). The influence of coarse aggregate content on compressive strength is seen in Figure 26 (a). CA content has a generally positive relationship with compressive strength. This trend was in line with a prior study, which revealed that when CA increases, so does HPC concrete strength. This is because greater CA leads to a more compact structure, which improves load-bearing capability and limits material deterioration [82-84]. Figure 26 (b) shows how compressive strength improves as cement content increases. This positive relationship between cement quantity and compressive strength is logical since higher C content causes greater binding due to enhanced cement component reactivity, although durability can be reduced, which can be managed by adding supplemental cementitious materials. Golfashani et al. investigation yielded similar results [44]. Concrete with a lower water-binder ratio will impart high strength, which is a universal requirement for all concrete types. The rationale behind this is that the higher value of W/B will introduce more air voids whereby less compact the concrete skeleton will form, decreasing the strength [82, 85]. In Figure 26 (c), we see a similar pattern in our optimized ANN-GA model.

Figure 26 (d) demonstrates the variation in compressive strength with concrete age, which indicates a positive connection. Figure 26 (e) depicts the relationship between strength and super-plasticizer amount. Although increasing the superplasticizer dosage may improve compressive strength, the amount used should be controlled since overdosing on SP will result in segregation and bleeding, which will impair compressive strength. Overloading the amount of SP will also influence concrete cohesiveness and homogeneity [86, 87].

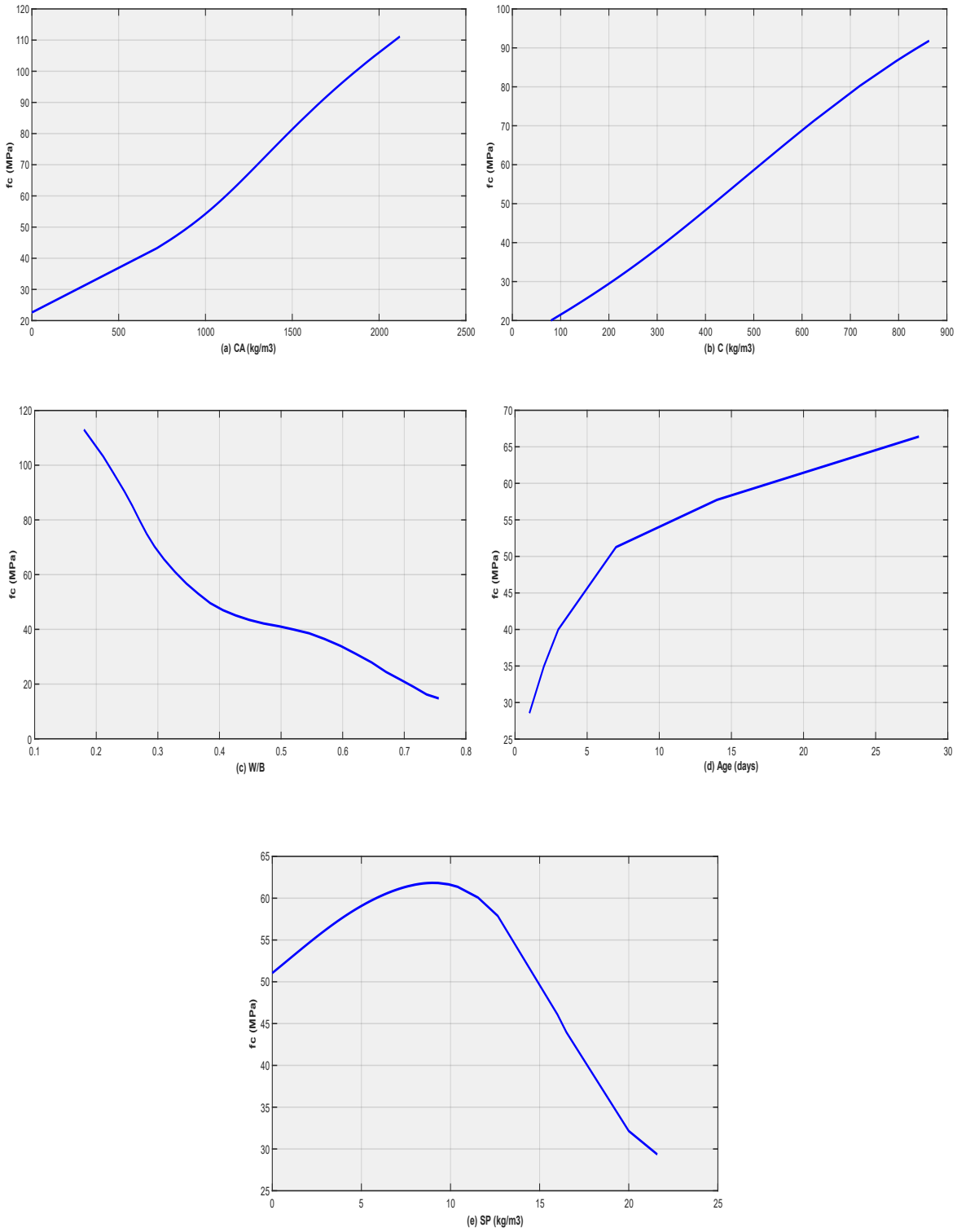

Figure 26 Partial Dependence Plot for (a) CA [kg/m3], (b) C [kg/m3], (c) W/B [kg/m3], (d) Age [days], (e) SP [kg/m3]

5.4 Validation of Model Via Experiments

Concrete mixture cylindrical specimens were examined according to the test method defined in ASTM C39 [88]. The samples are cured in water for 1, 3, 7, 14, and 28 days which are then taken out for testing. At each age, three samples were evaluated, and the average was used to determine the mean compressive strength (f_c). As capping of samples is necessary to smoothen the surface and to have uniform load application, therefore it was done using lime before testing. The tests were performed under compression testing was performed (CTM) and all the samples centered appropriately in the machine before applying load. Each mix design is tested for the required curing period, and 20 compressive strength values at different ages were obtained for the model prediction comparison.

Their testing results are shown in Table 8. Following the experimentation, the findings of the experiments are compared to the proposed model. Table 8 displays experimental test results, the model projected values and error values. Along with the specimen Id, I-1, the specimen's testing age is indicated where 1 refers to specimen I-1, which was evaluated 1 day after curing. The findings are presented using a scatter plot, as shown in Table 8, with the x-axis representing the data points and the y-axis representing the error values. The error is dispersed, as seen by the scatter figure, and the error range is 5 MPa.

Table 8 Comparison of Values Obtained from Experiment and Model

Sr #	Mix ID	Experimental	ANN-GA Model	Error (MPa)
1	I-1.1	21.5	20.93	0.57
2	I-1.3	29.1	31.48	-2.38
3	I-1.7	47.4	45.16	2.24
4	I-1.14	54.3	56.2	-1.9
5	I-1.28	62.8	60.71	2.09
6	I-2.1	26.9	25.75	1.15
7	I-2.3	31.6	33.9	-2.3
8	I-2.7	43.3	41.72	1.58
9	I-2.14	52.5	46.92	5.58
10	I-2.28	70.8	68.83	1.97
11	I-3.1	31.2	35.33	-4.13
12	I-3.3	38.7	40.91	-2.21
13	I-3.7	45.7	45.17	0.53
14	I-3.14	53.4	46.66	6.74
15	I-3.28	66.2	67.95	-1.75
16	I-4.1	14.9	12.24	2.66
17	I-4.3	22.3	24.34	-2.04
18	I-4.7	36.7	37.9	-1.2
19	I-4.14	52.4	55.97	-3.57
20	I-4.28	68.5	67.23	1.27

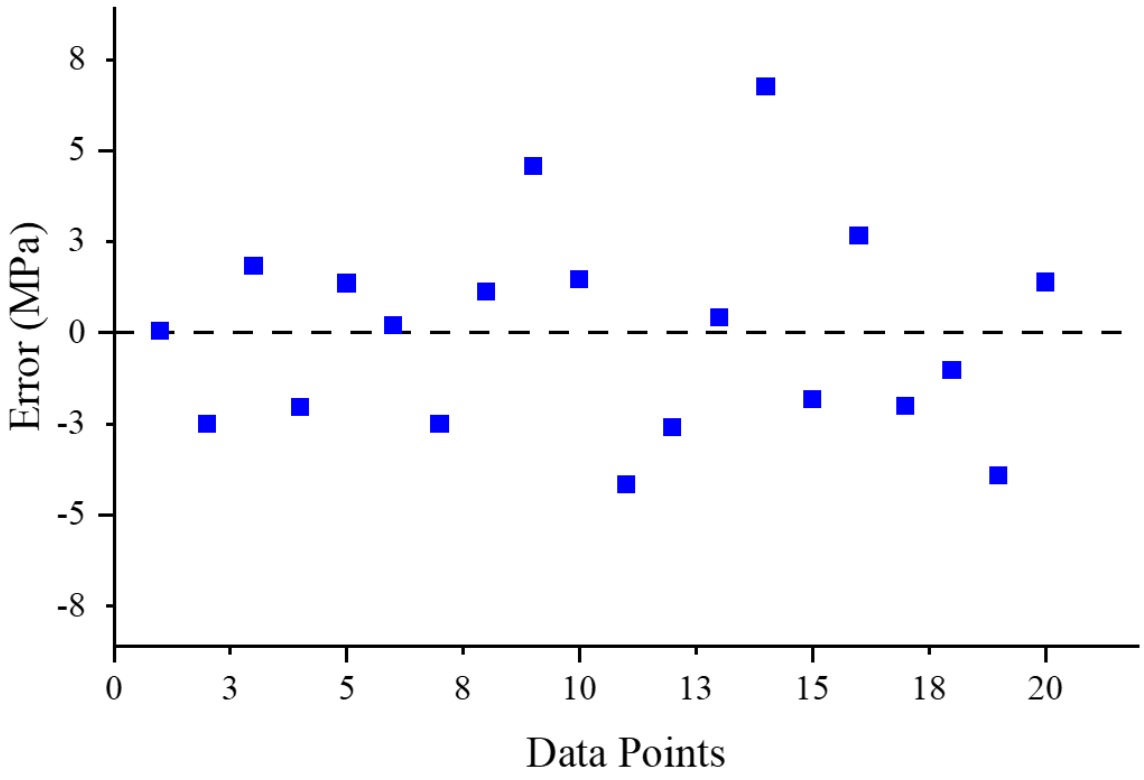

Figure 27 Error Distribution Plot of the Datapoints

5.5 Computer Software Package

Finally, utilizing the hybrid model (ANN-GA) a simple but convenient tool in the form of a graphical user interface (GUI) is developed in MATLAB. This GUI can be used for the estimation of HESC compressive strength. This will make it easier to use the ANN-GA model in practice. In order to obtain the predicted values of compressive strength, the user would only require giving inputs of parameters in the GUI as shown in Figure 28**.** A help button has been introduced to instruct the users on how to use the GUI (Figure 29).

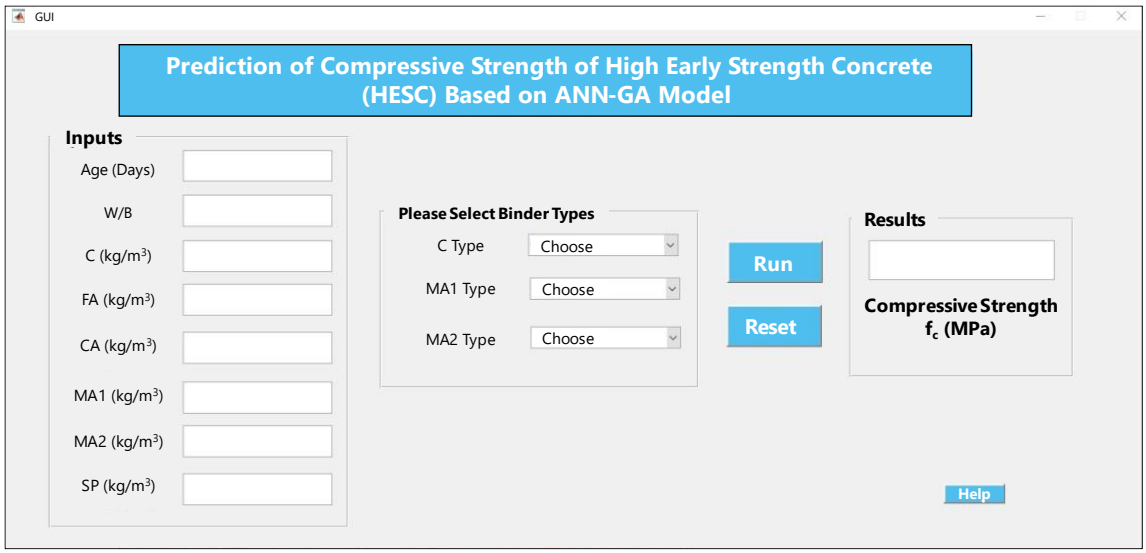

Figure 28 User-Friendly Graphical User Interface for the ANN-GA Model

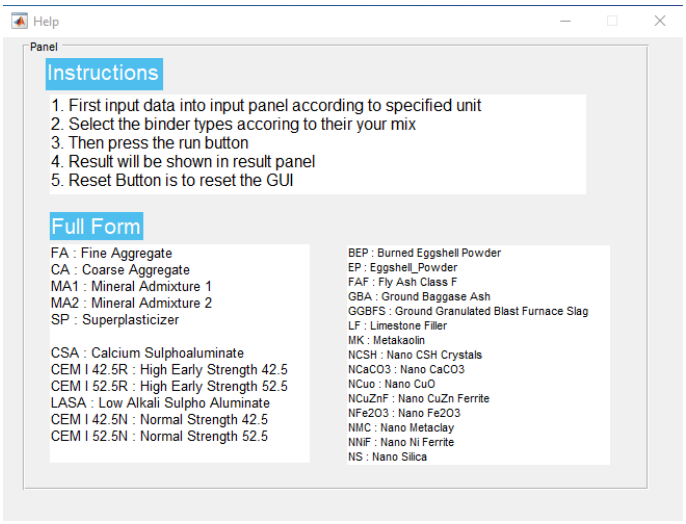

Figure 29 Interface of Help Button for User Convenience

Chapter 6

CONCLUSIONS AND RECOMMENDATIONS

6.1 Conclusions

The need for HESC has increased in the wake of the COVID-19 pandemic. Time and money can be saved by using accurate and trustworthy models to forecast the compressive strength of HESC. This study aims to develop a machine learning model utilizing ANN, for the HESC compressive strength prediction comprising various supplementary cementitious materials. The genetic algorithm was combined with the ANN approach to improving it, with GA selecting the best ANN architecture. Various input parameters have been selected for the model development which includes both numeric and categorical types. Two categories of mineral admixtures and cement types are used as categorical while the rest are used s numeric which include the amount of cement, superplasticizer, mineral admixture, coarse, fine aggregate, and water-binder ratio. The only output parameter was HESC's compressive strength.

The results of this study showed that the created model is effective at representing the highly nonlinear compressive strength response, as evidenced by high $R = 0.987$, $R^2 = 0.975$, and low values of RMSE = 4.05, and MAE = 3.14. The generated model's performance was the best among the developed machine learning models, demonstrating that the combination of GA and ANN produces the best results in terms of performance indices. The most critical criteria were cement quantity and water to binder ratio, with the mineral admixture-2 type being the least important. ANN-GA model performance is good with parameter variation, according to PDP analysis. The model's performance in real-time testing was tested during experimental validation. As a result, the created model can be utilized to forecast the compressive strength of HESC accurately using various parameters, thereby saving time and money.

6.2 Recommendations

The following are some of the research study recommendations.

- Other forms of concretes, such as ultra-high-performance concrete and fiber reinforced concrete, can be predicted using the suggested framework.
- Other properties of concrete, such as modulus of elasticity and tensile strength, can also be predicted using this framework.

References

[1] E. Benhelal, E. Shamsaei, and M. I. Rashid, "Challenges against CO2 abatement strategies in cement industry: A review," *J Environ Sci (China)*, vol. 104, pp. 84-101, Jun 2021.

[2] E. M. Golafshani, A. Behnood, and M. Arashpour, "Predicting the compressive strength of normal and High-Performance Concretes using ANN and ANFIS hybridized with Grey Wolf Optimizer," *Construction and Building Materials*, vol. 232, 2020.

[3] B. K. Steven H. Kosmatka, and William C. Panarese, *Design and Control of Concrete Mixtures- EB001*, FOURTEENTH EDITION ed. Portland Cement Association (PCA), 2008.

[4] Y. Kim, A. Hanif, M. Usman, M. J. Munir, S. M. S. Kazmi, and S. Kim, "Slag waste incorporation in high early strength concrete as cement replacement: Environmental impact and influence on hydration & durability attributes," *Journal of Cleaner Production*, vol. 172, pp. 3056-3065, 2018.

[5] D. Shen, C. Liu, J. Jiang, J. Kang, and M. Li, "Influence of super absorbent polymers on early-age behavior and tensile creep of internal curing high strength concrete," *Construction and Building Materials*, vol. 258, 2020.

[6] A. Alsharef, S. Banerjee, S. M. J. Uddin, A. Albert, and E. Jaselskis, "Early Impacts of the COVID-19 Pandemic on the United States Construction Industry," *International Journal of Environmental Research and Public Health*, vol. 18, no. 4, p. 1559, 2021.

[7] T.-B. Min, I.-S. Cho, W.-J. Park, H.-K. Choi, and H.-S. Lee, "Experimental study on the development of compressive strength of early concrete age using calcium-based hardening accelerator and high early strength cement," *Construction and Building Materials*, vol. 64, pp. 208-214, 2014.

[8] H. Al-musawi, F. P. Figueiredo, S. A. Bernal, M. Guadagnini, and K. Pilakoutas, "Performance of rapid hardening recycled clean steel fibre materials," *Construction and Building Materials*, vol. 195, pp. 483-496, 2019.

[9] Y. Guan, Y. Gao, R. Sun, M. C. Won, and Z. Ge, "Experimental study and field application of calcium sulfoaluminate cement for rapid repair of concrete pavements," *Frontiers of Structural and Civil Engineering*, vol. 11, no. 3, pp. 338-345, 2017.

[10] Z. Sha, X. Long, J. Feng, H. Jiang, and T. Wang, "Development of a fast-hardening retarding high-early-strength concrete with low-alkalinity sulphoaluminate cement and practical application," *Advances in Bridge Engineering*, vol. 1, no. 1, 2020.

[11] N. M. Alderete, A. M. Joseph, P. Van den Heede, S. Matthys, and N. De Belie, "Effective and sustainable use of municipal solid waste incineration bottom ash in concrete regarding strength and durability," *Resources, Conservation and Recycling*, vol. 167, 2021.

[12] M. McCarthy and R. Dhir, "Development of high volume fly ash cements for use in concrete construction," *Fuel*, vol. 84, no. 11, pp. 1423-1432, 2005.

[13] M. Amin and K. Abu el-hassan, "Effect of using different types of nano materials on mechanical properties of high strength concrete," *Construction and Building Materials*, vol. 80, pp. 116-124, 2015.

[14] A. Khaloo, M. H. Mobini, and P. Hosseini, "Influence of different types of nano-SiO2 particles on properties of high-performance concrete," *Construction and Building Materials*, vol. 113, pp. 188-201, 2016.

[15] M.-H. Zhang, J. Islam, and S. Peethamparan, "Use of nano-silica to increase early strength and reduce setting time of concretes with high volumes of slag," *Cement and Concrete Composites,* vol. 34, no. 5, pp. 650-662, 2012.
[16] D. Shen, X. Shi, S. Zhu, X. Duan, and J. Zhang, "Relationship between tensile Young's modulus and strength of fly ash high strength concrete at early age," *Construction and Building Materials,* vol. 123, pp. 317-326, 2016.
[17] J. Sun, X. Shen, G. Tan, and J. E. Tanner, "Modification Effects of Nano-SiO2 on Early Compressive Strength and Hydration Characteristics of High-Volume Fly Ash Concrete," *Journal of Materials in Civil Engineering,* vol. 31, no. 6, 2019.
[18] F. Ghasemzadeh, S. Sajedi, M. Shekarchi, H. Layssi, and M. Hallaji, "Performance Evaluation of Different Repair Concretes Proposed for an Existing Deteriorated Jetty Structure," *Journal of Performance of Constructed Facilities,* vol. 28, no. 4, 2014.
[19] M.-H. Zhang and J. Islam, "Use of nano-silica to reduce setting time and increase early strength of concretes with high volumes of fly ash or slag," *Construction and Building Materials,* vol. 29, pp. 573-580, 2012.
[20] S. W. M. Supit and F. U. A. Shaikh, "Durability properties of high volume fly ash concrete containing nano-silica," *Materials and Structures,* vol. 48, no. 8, pp. 2431-2445, 2014.
[21] M. S. M. Norhasri, M. S. Hamidah, and A. M. Fadzil, "Applications of using nano material in concrete: A review," *Construction and Building Materials,* vol. 133, pp. 91-97, 2017.
[22] K. P. Bautista-Gutierrez, A. L. Herrera-May, J. M. Santamaria-Lopez, A. Honorato-Moreno, and S. A. Zamora-Castro, "Recent Progress in Nanomaterials for Modern Concrete Infrastructure: Advantages and Challenges," *Materials (Basel),* vol. 12, no. 21, Oct 29 2019.
[23] R. A. Mahmood and N. U. Kockal, "Nanoparticles used as an ingredient in different types of concrete," *SN Applied Sciences,* vol. 3, no. 5, 2021.
[24] H. Bahadori and P. Hosseini, "Reduction of Cement Consumption by the Aid of Silica Nano-Particles (Investigation on Concrete Properties)," *Journal of Civil Engineering and Management,* vol. 18, no. 3, pp. 416-425, 2012.
[25] M.-C. Kang, D.-Y. Yoo, and R. Gupta, "Machine learning-based prediction for compressive and flexural strengths of steel fiber-reinforced concrete," *Construction and Building Materials,* vol. 266, p. 121117, 2021.
[26] Y. Wang, H. Zhang, Y. Geng, Q. Wang, and S. Zhang, "Prediction of the elastic modulus and the splitting tensile strength of concrete incorporating both fine and coarse recycled aggregate," *Construction and Building Materials,* vol. 215, pp. 332-346, 2019.
[27] T. Han, A. Siddique, K. Khayat, J. Huang, and A. Kumar, "An ensemble machine learning approach for prediction and optimization of modulus of elasticity of recycled aggregate concrete," *Construction and Building Materials,* vol. 244, p. 118271, 2020.
[28] L. Chen, C.-H. Kou, and S.-W. Ma, "Prediction of slump flow of high-performance concrete via parallel hyper-cubic gene-expression programming," *Engineering Applications of Artificial Intelligence,* vol. 34, pp. 66-74, 2014.
[29] S. Ray, M. Haque, M. M. Rahman, M. N. Sakib, and K. Al Rakib, "Experimental investigation and SVM-based prediction of compressive and splitting tensile strength of ceramic waste aggregate concrete," *Journal of King Saud University - Engineering Sciences,* 2021.
[30] F. Farooq *et al.*, "A Comparative Study for the Prediction of the Compressive Strength of Self-Compacting Concrete Modified with Fly Ash," *Materials (Basel),* vol. 14, no. 17, Aug 30 2021.

[31] A. I. Muhammad Nasir Amin , Kaffayatullah Khan, Muhammad Faisal Javed,Faisal I. Shalabi and Muhammad Ghulam Qadir "Comparison of Machine Learning Approaches with Traditional Methods for Predicting the Compressive Strength of Rice Husk Ash Concrete," *Crystals*, 2021.
[32] B. A. Salami, T. Olayiwola, T. A. Oyehan, and I. A. Raji, "Data-driven model for ternary-blend concrete compressive strength prediction using machine learning approach," *Construction and Building Materials*, vol. 301, 2021.
[33] U. K. Sevim, H. H. Bilgic, O. F. Cansiz, M. Ozturk, and C. D. Atis, "Compressive strength prediction models for cementitious composites with fly ash using machine learning techniques," *Construction and Building Materials*, vol. 271, 2021.
[34] H. Song *et al.*, "Predicting the compressive strength of concrete with fly ash admixture using machine learning algorithms," *Construction and Building Materials*, vol. 308, 2021.
[35] I. C. Yeh, "Modeling of strength of high-performance concrete using artificial neural networks," *Cement and Concrete Research*, vol. 28, no. 12, pp. 1797-1808, 1998.
[36] Q. Han, C. Gui, J. Xu, and G. Lacidogna, "A generalized method to predict the compressive strength of high-performance concrete by improved random forest algorithm," *Construction and Building Materials*, vol. 226, pp. 734-742, 2019.
[37] U. Anyaoha, A. Zaji, and Z. Liu, "Soft computing in estimating the compressive strength for high-performance concrete via concrete composition appraisal," *Construction and Building Materials*, vol. 257, 2020.
[38] M. R. Kaloop, D. Kumar, P. Samui, J. W. Hu, and D. Kim, "Compressive strength prediction of high-performance concrete using gradient tree boosting machine," *Construction and Building Materials*, vol. 264, 2020.
[39] D. Chakraborty, I. Awolusi, and L. Gutierrez, "An explainable machine learning model to predict and elucidate the compressive behavior of high-performance concrete," *Results in Engineering*, vol. 11, 2021.
[40] M. M. Hameed, M. K. AlOmar, W. J. Baniya, and M. A. AlSaadi, "Incorporation of artificial neural network with principal component analysis and cross-validation technique to predict high-performance concrete compressive strength," *Asian Journal of Civil Engineering*, vol. 22, no. 6, pp. 1019-1031, 2021.
[41] N.-D. Hoang, A.-D. Pham, Q.-L. Nguyen, and Q.-N. Pham, "Estimating Compressive Strength of High Performance Concrete with Gaussian Process Regression Model," *Advances in Civil Engineering*, vol. 2016, pp. 1-8, 2016.
[42] Y. Yu, W. Li, J. Li, and T. N. Nguyen, "A novel optimised self-learning method for compressive strength prediction of high performance concrete," *Construction and Building Materials*, vol. 184, pp. 229-247, 2018.
[43] D.-K. Bui, T. Nguyen, J.-S. Chou, H. Nguyen-Xuan, and T. D. Ngo, "A modified firefly algorithm-artificial neural network expert system for predicting compressive and tensile strength of high-performance concrete," *Construction and Building Materials*, vol. 180, pp. 320-333, 2018.
[44] E. Mohammadi Golafshani, M. Arashpour, and A. Behnood, "Predicting the compressive strength of green concretes using Harris hawks optimization-based data-driven methods," *Construction and Building Materials*, vol. 318, 2022.
[45] O. Theobald, *Machine Learning for Absolute Beginners A Plain English Introduction*, Third ed. Scatter Press, 2021.
[46] A. A. Shahmansouri, M. Yazdani, S. Ghanbari, H. Akbarzadeh Bengar, A. Jafari, and H. Farrokh Ghatte, "Artificial neural network model to predict the compressive strength of eco-friendly geopolymer concrete incorporating silica fume and natural zeolite," *Journal of Cleaner Production*, vol. 279, 2021.

[47] K. G. Kapanova, I. Dimov, and J. M. Sellier, "A genetic approach to automatic neural network architecture optimization," *Neural Computing and Applications*, vol. 29, no. 5, pp. 1481-1492, 2016.
[48] Z. Cömert and A. Kocamaz, "A Study of Artificial Neural Network Training Algorithms for Classification of Cardiotocography Signals," *Bitlis Eren University Journal of Science and Technology*, vol. 7, no. 2, pp. 93-103, 2017.
[49] J. H. Holland, *Adaptation in Natural and Artificial Systems*. MIT: The MIT Press, 1992.
[50] C.-H. Lim, Y.-S. Yoon, and J.-H. Kim, "Genetic algorithm in mix proportioning of high-performance concrete," *Cement and Concrete Research*, vol. 34, no. 3, pp. 409-420, 2004.
[51] M. C. N. C. N. R. M. A. Jayaram, "Elitist Genetic Algorithm Models_ Optimization of High Performance Concrete Mixes," *Taylor and Francis Online*, 2009.
[52] S. Katoch, S. S. Chauhan, and V. Kumar, "A review on genetic algorithm: past, present, and future," *Multimed Tools Appl*, pp. 1-36, Oct 31 2020.
[53] S. M. Mousavi, P. Aminian, A. H. Gandomi, A. H. Alavi, and H. Bolandi, "A new predictive model for compressive strength of HPC using gene expression programming," *Advances in Engineering Software*, vol. 45, no. 1, pp. 105-114, 2012.
[54] M. F. Iqbal *et al.*, "Prediction of mechanical properties of green concrete incorporating waste foundry sand based on gene expression programming," *J Hazard Mater*, vol. 384, p. 121322, Feb 15 2020.
[55] S. Cangiano, A. Meda, and G. A. Plizzari, "Rapid hardening concrete for the construction of a small span bridge," *Construction and Building Materials*, vol. 23, no. 3, pp. 1329-1337, 2009.
[56] M. Batog, "SELF-COMPACTING CONCRETE WITH CEM II/A-S 52,5N AND HIGH FLY ASH ADDITION IN PRECAST ELEMENTS PRODUCTION," *International Journal of Research in Engineering and Technology*, 2014.
[57] A. Ghazy, M. T. Bassuoni, and A. Shalaby, "Nano-Modified Fly Ash Concrete: A Repair Option for Concrete Pavements," *ACI Materials Journal*, 2016.
[58] Z. Wu, C. Shi, K. H. Khayat, and S. Wan, "Effects of different nanomaterials on hardening and performance of ultra-high strength concrete (UHSC)," *Cement and Concrete Composites*, vol. 70, pp. 24-34, 2016.
[59] M. N. Matthew Maler, and Nader Ghafoori, "Frost Resistance of High Early-Age Strength Concretes for Rapid Repair," presented at the 17th International Conference on Cold Regions Engineering, 2017.
[60] T. Guo, Y. Xie, and X. Weng, "Evaluation of the bond strength of a novel concrete for rapid patch repair of pavements," *Construction and Building Materials*, vol. 186, pp. 790-800, 2018.
[61] F. Han and Z. Zhang, "Hydration, mechanical properties and durability of high-strength concrete under different curing conditions," *Journal of Thermal Analysis and Calorimetry*, vol. 132, no. 2, pp. 823-834, 2018.
[62] M. S. M. Norhasri, M. S. Hamidah, and A. M. Fadzil, "Inclusion of nano metaclayed as additive in ultra high performance concrete (UHPC)," *Construction and Building Materials*, vol. 201, pp. 590-598, 2019.
[63] L. P. Singh, D. Ali, I. Tyagi, U. Sharma, R. Singh, and P. Hou, "Durability studies of nano-engineered fly ash concrete," *Construction and Building Materials*, vol. 194, pp. 205-215, 2019.
[64] A. Kaleta-Jurowska and K. Jurowski, "The Influence of Ambient Temperature on High Performance Concrete Properties," *Materials (Basel)*, vol. 13, no. 20, Oct 18 2020.

[65] T. Klathae, N. Tanawuttiphong, W. Tangchirapat, P. Chindaprasirt, P. Sukontasukkul, and C. Jaturapitakkul, "Heat evolution, strengths, and drying shrinkage of concrete containing high volume ground bagasse ash with different LOIs," *Construction and Building Materials,* vol. 258, 2020.
[66] C. Li and L. Jiang, "Utilization of limestone powder as an activator for early-age strength improvement of slag concrete," *Construction and Building Materials,* vol. 253, 2020.
[67] D. Shen, C. Wen, P. Zhu, Y. Wu, and J. Yuan, "Influence of Barchip fiber on early-age autogenous shrinkage of high strength concrete," *Construction and Building Materials,* vol. 256, 2020.
[68] M. Soutsos and F. Kanavaris, "Compressive strength estimates for adiabatically cured concretes with the Modified Nurse-Saul (MNS) maturity function," *Construction and Building Materials,* vol. 255, 2020.
[69] A. Teara and D. Shu Ing, "Mechanical properties of high strength concrete that replace cement partly by using fly ash and eggshell powder," *Physics and Chemistry of the Earth, Parts A/B/C,* vol. 120, 2020.
[70] H. H. Alqamish and A. K. Al-Tamimi, "Development and Evaluation of Nano-Silica Sustainable Concrete," *Applied Sciences,* vol. 11, no. 7, 2021.
[71] T. Fantu, G. Alemayehu, G. Kebede, Y. Abebe, S. K. Selvaraj, and V. Paramasivam, "Experimental investigation of compressive strength for fly ash on high strength concrete C-55 grade," *Materials Today: Proceedings,* vol. 46, pp. 7507-7517, 2021.
[72] Z. Zhou, M. Sofi, J. Liu, S. Li, A. Zhong, and P. Mendis, "Nano-CSH modified high volume fly ash concrete: Early-age properties and environmental impact analysis," *Journal of Cleaner Production,* vol. 286, 2021.
[73] *BS EN 197-1:2011, Part 1 Composition, specifications and conformity criteria for common cements*, 2011.
[74] *ASTM C618-08a Standard Specification for Coal Fly Ash and Raw or Calcined Natural Pozzolan for Use in Concrete*, 2008.
[75] *ASTM C1240-05 Standard Specification for Silica Fume Used in Cementitious Mixtures*, 2005.
[76] *ASTM C127-07 Standard Test Method for Density, Relative Density (Specific Gravity), and Absorption of Coarse Aggregate*, 2007.
[77] *ASTM C128-07 Standard Test Method for Density, Relative Density (Specific Gravity), and Absorption of Fine Aggregate*, 2007.
[78] A. Committee, "211.4R-08: Guide for Selecting Proportions for High-Strength Concrete Using Portland Cement and Other Cementitious Materials," *Technical Documents,* 12/1/2008 2008.
[79] F. Özcan, C. D. Atiş, O. Karahan, E. Uncuoğlu, and H. Tanyildizi, "Comparison of artificial neural network and fuzzy logic models for prediction of long-term compressive strength of silica fume concrete," *Advances in Engineering Software,* vol. 40, no. 9, pp. 856-863, 2009.
[80] H. Nguyen, T. Vu, T. P. Vo, and H.-T. Thai, "Efficient machine learning models for prediction of concrete strengths," *Construction and Building Materials,* vol. 266, 2021.
[81] Z. Ullah *et al.*, "A comparative study of machine learning methods for bio-oil yield prediction - A genetic algorithm-based features selection," *Bioresour Technol,* vol. 335, p. 125292, Sep 2021.
[82] A. Dushimimana, A. A. Niyonsenga, and F. Nzamurambaho, "A review on strength development of high performance concrete," *Construction and Building Materials,* vol. 307, 2021.

[83] W.-T. Lin, "Effects of sand/aggregate ratio on strength, durability, and microstructure of self-compacting concrete," *Construction and Building Materials,* vol. 242, 2020.
[84] L. Xu, F. Wu, Y. Chi, P. Cheng, Y. Zeng, and Q. Chen, "Effects of coarse aggregate and steel fibre contents on mechanical properties of high performance concrete," *Construction and Building Materials,* vol. 206, pp. 97-110, 2019.
[85] E. H. Kadri, S. Aggoun, S. Kenai, and A. Kaci, "The Compressive Strength of High-Performance Concrete and Ultrahigh-Performance," *Advances in Materials Science and Engineering,* vol. 2012, pp. 1-7, 2012.
[86] S. A. M. Muhsen Salam Mohammed, Megat Azmi Megat Johari, "Influence of Superplasticizer Compatibility on the Setting Time, Strength and Stiffening Characteristics of Concrete," *Advances in Applied Sciences,* 2016.
[87] W. Xun, C. Wu, X. Leng, J. Li, D. Xin, and Y. Li, "Effect of Functional Superplasticizers on Concrete Strength and Pore Structure," *Applied Sciences,* vol. 10, no. 10, 2020.
[88] *ASTM C39C/39M-05 Standard Test Method for Compressive Strength of Cylindrical Concrete Specimens*, 2005.